

A PAN-STARRS + UKIDSS SEARCH FOR YOUNG, WIDE PLANETARY-MASS COMPANIONS IN UPPER SCORPIUS

KIMBERLY M. ALLER^{1,2}, ADAM L. KRAUS^{1,3}, MICHAEL C. LIU¹, WILLIAM S. BURGETT¹, KENNETH C. CHAMBERS¹, KLAUS W. HODAPP¹, NICK KAISER¹, EUGENE A. MAGNIER¹, PAUL A. PRICE⁴

ABSTRACT

We have combined optical and NIR photometry from Pan-STARRS 1 and UKIDSS to search the young (5–10 Myr) star-forming region of Upper Scorpius for wide (≈ 400 –4000 AU) substellar companions down to $\sim 5 M_{Jup}$. Our search is ≈ 4 mag deeper than previous work based on 2MASS. We identified several candidates around known stellar members using a combination of color selection and spectral energy distribution fitting. Our followup spectroscopy has identified two new companions as well as confirmed two companions previously identified from photometry, with spectral types of M7.5–M9 and masses of ~ 15 –60 M_{Jup} , indicating a frequency for such wide substellar companions of $\sim 0.6 \pm 0.3\%$. Both USco 1610–1913B and USco 1612–1800B are more luminous than expected for their spectral type compared with known members of Upper Sco. HIP 77900B has an extreme mass ratio ($M_2/M_1 \approx 0.005$) and an extreme separation of 3200 AU. USco 1602–2401B also has a very large separation of 1000 AU. We have also confirmed a low-mass stellar companion, USco 1610–2502B (730 AU, M5.5). Our substellar companions appear both non-coeval with their primary stars according to evolutionary models and, as a group, are systematically more luminous than the Upper Sco cluster sequence. One possible reason for these luminosity discrepancies could be different formation processes or accretion histories for these objects.

Subject headings:

1. INTRODUCTION

Recent advances in direct imaging techniques have led to the discovery of planets in moderately wide (~ 10 –100 AU) orbits around other stars, such as *Formalhaut* (Kalas et al. 2008), HR 8799 (Marois et al. 2008, 2010), and β Pic (Lagrange et al. 2009). Direct imaging surveys have also discovered planetary-mass ($\lesssim 13 M_{Jup}$) companions with very large (~ 200 –500 AU) orbital radii including 1RXS J1609–2105B (8 M_{Jup} , 330 AU; Lafrenière et al. 2008), CHXR 73B (12 M_{Jup} , 210 AU; Luhman et al. 2006), and GSC 06214–00210B (14 M_{Jup} , 330 AU; Ireland et al. 2011). The most extreme of such wide companions is WD 0608–661B with a mass of 7 M_{Jup} and a projected separation of 2500 AU (Luhman et al. 2011). It is difficult to determine whether a planetary-mass companion at such a large distance formed from a protoplanetary disk (and thus should be considered a planet) or as a binary system (and should be called a brown dwarf). Regardless of their origins, detailed spectroscopic and photometric analysis of these directly imaged systems (e.g. Lafrenière et al. 2008; Bowler et al. 2010) can yield insight into the properties (e.g. luminosity, temperature and mass) of gas-giant planets, and thereby shed light on the over 500 radial velocity and transiting exoplanets that lie within a few AU of their host stars and therefore cannot be directly studied.

Determining the mass function, separation distribution, and frequency of these wide planetary-mass companions will provide insight into their formation. The precise boundary between planets and brown dwarfs is still under debate. The most widely used definition adopts the deuterium-burning limit of $\approx 13 M_{Jup}$ (e.g. Spiegel et al. 2011) to set the boundary. Alternatively, the mass distribution of substellar companions might provide a means to distinguish planets from brown dwarfs, by shedding light on their formation process(es). The mass function of companions to solar-type stars has two distinct populations separated by a deficit of objects around $\sim 30 M_{Jup}$ (e.g. Lineweaver & Grether, 2005; a.k.a. the “brown dwarf desert”), suggesting that the population of objects with masses below this gap might have a common origin and thus all be considered planets.

Similarly, the distribution of separations might provide valuable clues. If wide substellar companions form like binary stars, we expect that they may reside at separations as large as ~ 1000 AU from their primary star, as stellar binaries are observed at such large separations. Such companions would represent the extreme low-mass end of binary star formation (Kratzer et al. 2010). Therefore we would expect that their separation distribution would be similar to that for stars and brown dwarfs (Kraus et al. 2011) such that their distribution would be logarithmically flat (i.e. companion masses are equally likely in $\log(\text{separation})$). If instead wide substellar companions form like planets, we do not expect to find them beyond a few hundred AU, because protoplanetary disks should not form planets so far out. Dodson-Robinson et al. (2009) find that even planet formation in moderately wide orbits (35–100 AU), such as in the case of HR 8799, could not have formed via core accretion. Whether or not the competing disk-instability

¹ University of Hawaii, Institute of Astronomy

² Visiting Astronomer at the Infrared Telescope Facility, which is operated by the University of Hawaii under Cooperative Agreement no. NNX-08AE38A with the National Aeronautics and Space Administration, Science Mission Directorate, Planetary Astronomy Program.

³ Harvard-Smithsonian Center for Astrophysics, 60 Garden Street, Cambridge, MA 02138, USA

⁴ Department of Astrophysical Sciences, Princeton University, Princeton, NJ 08544, USA

model (Boss 2001) can form planets at such large separations has not been well explored. Disks have only been modeled to moderate radii (300 AU; e.g. Kratter et al. 2010; Meru & Bate 2010). In addition, the typical sizes of circumstellar disks range from ~ 100 –400 AU (Vicente & Alves 2005), making in situ formation by disk-instability at very wide separations, where there is no disk at all, unlikely.

Substellar and planetary-mass companions are expected to cool and fade quickly after their formation and therefore are most readily detected in young ($\lesssim 10$ Myr) star-formation regions. We have used the UKIDSS Galactic Cluster Survey (GCS) and the Pan-STARRS 1 (PS1) 3π Survey to search for wide planetary-mass companions in the Upper Sco association. A similar search has previously been conducted with 2MASS (Kraus & Hillenbrand 2007a), but the 2MASS detection limit ($K = 14.3$; $\sim 20 M_{Jup}$ in Upper Sco) is ~ 4 mag brighter than for UKIDSS ($K = 18.2$; $\sim 5 M_{Jup}$ in Upper Sco). Combining both optical (PS1) and NIR (UKIDSS) data increases the wavelength coverage, significantly improving the ability to reject reddened background stars as potential planetary-mass companions. In Section 2 we discuss the UKIDSS GCS and the PS1 photometric data. In Section 3 we describe our search method and how we photometrically determine the spectral type of our candidates. In Section 4 we describe the spectroscopic followup and our new substellar and a low-mass stellar companions. Our discussion is in Section 5 and our conclusions are in Section 6.

2. SURVEY DATA

2.1. UKIDSS

The United Kingdom Infrared Deep Sky Survey (UKIDSS) began in 2005 and uses the 3.8 m United Kingdom Infrared Telescope (UKIRT) located on Mauna Kea (Skrutskie et al. 2006). The UKIDSS project is defined in Lawrence et al. (2007). UKIDSS uses the UKIRT Wide Field Camera (WFCAM; Casali et al. 2007) and a photometric system described in Hewett et al. (2006). The pipeline processing and science archive are described in Irwin et al. (2004) and Hambly et al. (2008). UKIDSS consists of five surveys: the Galactic Clusters Survey (GCS), the Large Area Survey (LAS), the Galactic Plane Survey (GPS), the Ultra-Deep Survey (UDS) and the Deep Extragalactic Survey (DXS). The GCS covers $\approx 1400 \text{ deg}^2$ of galactic star-formation regions and open clusters visible from the Northern Hemisphere ($\delta \gtrsim -30^\circ$), including the Upper Sco star-forming region, in 5 NIR bands, *ZYJHK* (≈ 0.8 – $2.4 \mu\text{m}$) (Lawrence et al. 2007). This survey is only $\sim 40\%$ complete (by area) and the 5σ limiting magnitudes (Vega) in the observed area are $Z = 20.4$, $Y = 20.1$, $J = 19.6$, $H = 18.8$, and $K = 18.2$ mag⁵. In addition, we use data from the other UKIDSS surveys (LAS, UDS, and DXS) to construct stellar spectral energy (SED) templates of known dwarfs in order to estimate the spectral type of our candidates. See Section 3.2, Section 3.3, and Appendix A for more details.

For both our wide companion search and ultracool dwarf template construction, we use the catalog data

from the UKIDSS DR9 release. Also, all UKIDSS magnitudes are on the Vega system. We chose good data as having the following properties: magnitude errors ≤ 0.2 mag, not deblended and without saturated, almost-saturated or bad pixels. These requirements remove most of the spurious detections we may encounter near bright stars. Furthermore, we ignore all detections $< 1''$ from the location of our primary star because they likely correspond either to the actual primary star or small artifacts within the star’s point spread function (PSF). We note that our completeness within $3''$ from the primary star is still very low because any companion would be likely to be contaminated by the relatively brighter primary star’s PSF.

2.2. Pan-STARRS 1

Pan-STARRS 1 (PS1) is a 1.8 m, wide-field telescope located on Haleakalā on the island of Maui, conducting a multi-wavelength, multi-epoch, optical imaging survey (Kaiser et al. 2002). Its large sky coverage ($\approx 30,000 \text{ deg}^2$) coupled with its z_{P1} ($\lambda_{eff} = 866 \text{ \AA}$) and y_{P1} ($\lambda_{eff} = 962 \text{ \AA}$) filters provide both coverage of the same star-forming regions as UKIDSS and greater sensitivity at longer wavelengths, where brown dwarf and young gas giant planet spectra are brighter compared to the shorter wavelengths. Our work is the first to use PS1 data to search for young brown dwarfs and planetary-mass companions.

We use data from the PS1 3π survey, which began in 2010, both to search for candidate companions and to construct spectral energy distribution templates of ultracool dwarfs (see Section 3.2, Section 3.3, and Appendix A). The 3π Survey covers $\approx 75\%$ of the sky in 5 optical filters, g_{P1} , r_{P1} , i_{P1} , z_{P1} , and y_{P1} (Tonry et al. 2012). At each epoch a single field is exposed for 43 s in g_{P1} , 40 s in r_{P1} , 45 s in i_{P1} , 30 s in z_{P1} , and 30 s in y_{P1} . The photometry from the reduced multi-epoch data have been averaged to calculate mean magnitudes. The predicted final limiting magnitudes, on the AB system, for each filter are 23.4, 22.8, 22.2, 21.6, and 20.1 mag in g_{P1} , r_{P1} , i_{P1} , z_{P1} , and y_{P1} , respectively (Dupuy & Liu 2009; Tonry et al. 2012).

We chose good quality data according to the photometric quality flags set in the PS1 Desktop Virtual Observatory (DVO) database (Magnier 2006). We queried the DVO catalogs for 3π survey and selected objects with the following attributes: fits a PSF model (is not extended); is not saturated; has a good sky measurement; is not likely a cosmic ray, a diffraction spike, a ghost or a glint; does not lie between the image chips; and has the quality flag `psf_qf` ≥ 0.9 to ensure that at least 90% of the object is unmasked. Furthermore, we require objects to be detected at least twice in a single night in at least one of the five filters to remove potential spurious sources that would only appear as single detections. Finally, we require that a single bandpass measurement error be ≤ 0.2 mag in order to use that bandpass. We note that we obtained photometry from the PS1 database prior to the updated photometric calibrations (Schlafly et al. 2012). Because the previous database had misreported some photometric errors as below 0.01 mag, we have capped the reported photometric error at 0.01 mag. All PS1 photometry tabulated is from

⁵ http://surveys.roe.ac.uk/wsa/dr9plus_release.html

the previous database, for consistency with our actual search and analysis.

3. CANDIDATE SELECTION

We combined the UKIDSS GCS and PS1 3π catalogs to search for objects located within $1\text{--}30''$ of known Upper Sco members using TOPCAT⁶ (Taylor 2005). Bona fide members are taken from de Geus et al. (1989), Kunkel (1999), Walter et al. (1994), de Zeeuw et al. (1999), Ardila et al. (2000), Preibisch et al. (2002), Martín et al. (2004), Lodieu et al. (2006), Slesnick et al. (2008) and Rizzuto et al. (2011). Kraus & Hillenbrand (2007a) compiles these lists for all members determined prior to the paper. Our final input list includes 673 spectroscopically confirmed Upper Sco members.

The decreased detection efficiency within $3''$ limits our search to companions with projected separations greater than ~ 400 AU. Furthermore, the UKIDSS K -band sensitivity can detect companions down to $\sim 5 M_{Jup}$, assuming an age of $5\text{--}10$ Myr for Upper Sco (Chabrier et al. 2000).

3.1. Color Selection

Our initial candidate selection used NIR colors to isolate candidates that lie along the Upper Sco color-magnitude sequence. This significantly reduces the obvious background objects with neutral colors. We then selected substellar candidates using UKIDSS H and K photometry, which are nearly complete for Upper Sco. Our candidates were selected to lie above a diagonal line which roughly traces the cluster sequence and to be fainter than $H = 12$ ($\sim 90 M_{Jup}$; Chabrier et al. 2000). All companions brighter than this limit should have been detected by Kraus & Hillenbrand (2009b). We empirically defined this line by horizontally shifting the evolutionary model tracks until they bracketed the edge of the observed primary star sequence (Figure 1).

3.2. Spectral Types from SED Fitting

These initial color-selected candidates were then fit using our SED template library to estimate their spectral type. See Appendix A for a description of our SED templates. We performed a χ^2 minimization to determine the spectral type using the available PS1 and UKIDSS photometry for each of our candidates. Our χ^2 minimization took into account uncertainties in both the candidate data and the templates using the following weight, w_i for each filter, i :

$$w_i = (\sigma_{obs,i}^2 + \sigma_{SED,i}^2)^{-1} \quad (1)$$

where $\sigma_{obs,i}$ is the magnitude error in the candidate data and $\sigma_{SED,i}$ is the magnitude error in the SED template. We set the magnitude error in the SED templates to a constant value of 0.1 mag in order to prevent the SED template with the largest uncertainties (i.e. those constructed by averaging open cluster or Upper Sco members) from returning the minimum χ^2 . This was an issue because the individual photometric uncertainties are ~ 0.01 mag, whereas the photometric scatter within each spectral type in either the open clusters or Upper Sco is

around 0.5 mag. Then we calculated the distance modulus of each candidate relative to *each* SED template, DM_j , by minimizing the χ^2 for the distance:

$$DM_j = \frac{\sum_{i=0}^n w_i (m_{obs,i} - m_{SED,i,j})}{\sum_{i=0}^n w_i} \quad (2)$$

where j is the SED template, i is the filter, $m_{obs,i}$ is the observed magnitude in a filter, $m_{SED,i}$ is the magnitude of the SED template, n is the total number of filters, and w_i is the weight, from the previous equation.

Since the SED templates can have a different number of filters, we determined the reduced χ^2 between the candidate data and templates in order to compare the goodness of fit between different templates. We also required that each template have UKIDSS photometry because our initial color selection of candidates is done in the NIR. Therefore, our final χ^2 fitting matched the candidate data with all of the SED templates with any NIR photometry and measurements in at least three filters in common. We then determined the relative distance modulus to each of these SED templates (Equation 2) and the associated reduced χ^2 .

Finally, the best fit SED was chosen based on the minimum reduced χ^2 . The absolute magnitude to spectral type relations (see Appendix A) convert the relative distance modulus determined in our χ^2 fitting to an absolute scale.

3.3. Spectral Type Uncertainties

There is an uncertainty in the spectral type estimates from the SED fitting due to both the intrinsic scatter in the SEDs of field objects of a given spectral type and the measurement uncertainties in both the candidate data and the SED templates. To incorporate this uncertainty in our final distance estimate, we carried out a Monte Carlo simulation to find the distribution of best-fit templates. For each candidate, we perturbed the photometry in each filter by drawing from a Gaussian distribution corresponding to the magnitude errors. We varied the SED template photometry in the same manner. For each realization (out of a total of 5000), we recomputed the best-fit distance and spectral type, resulting in a distribution of best fit spectral type and distance. We generated 5000 iterations, because the median distance and spectral type from the ensemble of fits converged for a tested set of objects with a variety of measurement errors in y_{P1} .

The final best fit spectral type is the median from the Monte Carlo simulation and the best fit template is the most probable template (according to the Monte Carlo distribution) with that spectral type. Note that the SED fitting routine may select different SEDs with the same spectral type. Therefore, a spectral type uncertainty of zero only means that the object had best fitting SED templates with the same spectral type, not necessarily a single SED template. In these cases we adopted a spectral type uncertainty according to the available templates, usually approximately one spectral subclass. Furthermore, the spectral type estimates are quantized and thus we only have a total of 34 possible spectral types.

⁶ <http://www.starlink.ac.uk/topcat>

For our purposes, the spectral type uncertainty simply serves to further distinguish the quality of the template fit and an object’s candidacy.

3.4. Final Candidate Selection

We selected the final candidates combining the reduced χ^2 ($\chi^2_\nu < 5$) and spectral type cut ($> M7$) from the SED fitting, a visual check on the UKIDSS and/or PS1 images, and their observability with IRTF SpeX according to their magnitude ($J \lesssim 18$). Although the SED template fitting routine efficiently removes many of the reddened background stars that pass the initial NIR color selection, some still may pass. Our criteria will miss objects without at least three-band photometry, but it gives us a relatively pure candidate sample for followup spectroscopy in comparison to a solely color-selected one. We started with a total of 285 color-selected candidates. There were a total of 30 candidates remaining after the SED fitting for spectral type and our χ^2 cut.

4. RESULTS

4.1. Spectroscopic Followup

In principle proper motions could confirm candidates as comoving. However the predicted uncertainty in the UKIDSS proper motions is only $\sim 13 \text{ mas yr}^{-1}$. This precision is insufficient for Upper Sco because of its very low proper motion ($\mu_\alpha, \mu_\delta = -10, -25 \text{ mas yr}^{-1}$; de Zeeuw et al. 1999). Therefore, we require spectroscopy to confirm our candidates as true companions.

We obtained spectroscopic followup using SpeX (Rayner et al. 2003), a medium-resolution, near-IR spectrograph ($0.8\text{--}2.5 \mu\text{m}$) on the 3-meter NASA Infrared Telescope Facility (IRTF) on Mauna Kea. The low resolution (LowRes15) prism mode with a $0.8''$ slit ($R \equiv \lambda/\Delta\lambda \approx 100$) is well-suited to spectroscopic confirmation of our substellar companions which are expected to have spectral types of late-M to mid-L. Even at this low resolution, the spectra of substellar companions will have broad water band and molecular features that distinguish them from background stars. We can also easily distinguish a triangular H -band continuum, a feature which is characteristic of young low-mass objects (Lucas et al. 2001; Allers et al. 2007).

We observed a total of 6 candidates on 2011 June 19-22 (UT) in cloudy conditions with average seeing ($\sim 0.8''$). On 2012 July 5 we observed one candidate in poor seeing ($\sim 1.5''$). On July 7-8 we observed another 7 candidates in excellent seeing ($\sim 0.5''$). On 2013 April 16 we reobserved two companions to obtain higher signal-to-noise spectra. Each observation used the standard ABBA nod pattern for sky subtraction. We observed an A0V standard star following each candidate (with the exception of a few shared standards for nearby targets) then took wavelength and flatfield calibrations immediately afterward. We reduced the data using version 3.4 of the SpeXtool package (Vacca et al. 2003; Cushing et al. 2004). Table 1 tabulates the observation details.

4.2. Spectral Type

The spectral resolution ($R \approx 100$) is too low to determine the spectral type using gravity/age independent flux indices (Allers et al. 2007). Instead we first fit each spectrum to the a collection of ultracool dwarf spectra

in the IRTF/SpeX SpeX Prism Library ⁷. The adopted spectral type for our candidates is that of the best fitting object. We adopt a spectral type uncertainty of half a spectral subclass (e.g. $M9 \pm 0.5$) which encompasses both the uncertainty in the spectral type of the SpeX Prism Library objects and cases where the candidate may fit to more than one object.

In addition, we compared our candidates to optical M and L dwarf standards observed with IRTF/SpeX also in prism mode, a common method to determine spectral type in the NIR (e.g. Luhman et al. 2003; Muench et al. 2007). These M dwarf standards are from the spectral classification scheme of Kirkpatrick et al. (1991) and the L dwarf standards of Kirkpatrick et al. (1999). The M–L dwarf NIR spectral sequence in low resolution ($R \approx 100$) is characterized by water absorption at $1.4 \mu\text{m}$ and $1.8 \mu\text{m}$. Thus the H -band and K -band slopes change with spectral type. Comparisons with the M–L dwarf optical standards yield the same spectral type as comparisons with both the SpeX Prism Library and young M dwarfs, although there are discrepancies due to the youth of our companions. Figure 2 compares each of our companions with the M and L dwarf standards.

Finally, we compared our candidates to young M dwarfs from Muench et al. (2007) with spectral types straddling our candidates’ best fit spectral type from the Prism Library comparison. For each candidate, the best fitting young M dwarf is clearly the best match compared to the other young M dwarfs with a spectral type difference of just half a subclass. Therefore our adopted spectral type uncertainty of half a subclass is consistent. The final spectral type is that of the best matching young M dwarf. Our new companions have spectral types of M9, M9, M8.5, M7.5, and M5.5. We tabulate their properties in Table 2.

4.3. Companion Physical Properties

We calculated both the effective temperatures (T_{eff}) and the bolometric magnitudes (M_{bol}) of our companion discoveries and their primaries using empirical relationships from the literature. We adopted a spectral type uncertainty of half a subclass for all primary stars, except in the case of HIP 77900 where we assumed an uncertainty of one subclass. For all objects we performed a Monte Carlo simulation to derive the physical properties and their 68th percentile confidence limits. For each object, we perturbed its spectral type and the resulting T_{eff} by drawing from a Gaussian distribution corresponding to the uncertainty in each parameter. The T_{eff} has uncertainties due to both the spectral type uncertainties and the conversion from spectral type to T_{eff} . Our methods to calculate T_{eff} , M_{bol} , and mass are slightly different depending on the spectral type of the object.

For objects with spectral type $\geq M5$, we determined T_{eff} from the observed spectral type using the young M dwarf scale of Luhman et al. (2003). We note that the Luhman et al. (2003) scale is tailored for young stars and brown dwarfs, like our companions. For comparison, we also converted spectral type to T_{eff} using the Golimowski et al. (2004) relationship for old field dwarfs with spectral types later than M6 (with an uncertainty of 124K). We quote the T_{eff} values from both meth-

⁷ <http://pono.ucsd.edu/~adam/browndwarfs/spexprism>

ods in Table 2 and adopt an intrinsic T_{eff} uncertainty of 124 K for both conversions. The T_{eff} uncertainties in the table also take into account the uncertainty in spectral types. We used both T_{eff} values to determine the mass using the Chabrier et al. (2000) Lyon/DUSTY evolutionary models for both 5 Myr and 10 Myr, corresponding to the age range of Upper Sco. To compute bolometric luminosity, we used bolometric corrections as a function of spectral type from Golimowski et al. (2004) to convert from K -band magnitude to M_{bol} .

For stars with earlier spectral types (M0–M5), we used the empirical relationship between temperature and spectral type from Luhman et al. (2003) and then derived the mass using T_{eff} from the Baraffe et al. (1998) Lyon/NextGen evolutionary models. Then we used the spectral type to select the V -band bolometric corrections from Schmidt-Kaler (1982) and the photospheric $V - K$ color from Bessell & Brett (1988). We converted from the $V - K$ color to 2MASS K_S using the color transformation in Carpenter (2001). We then used these quantities with the observed K_S magnitude to calculate M_{bol} .

For the earliest type stars we used the calibrations between spectral type and T_{eff} from Schmidt-Kaler (1982) for spectral types of B8–K7 and from Kenyon & Hartmann (1995) for spectral types $< B8$. We then derived the mass using T_{eff} from the Siess et al. (2000) evolutionary models for both 5 and 10 Myr. We assumed a T_{eff} uncertainty of 100 K from the spectral type to T_{eff} conversion. We used the observed spectral type to select V -band bolometric corrections using relationships from Schmidt-Kaler (1982) for spectral types of B8–K7 and Kenyon & Hartmann (1995) for spectral types $< B8$. To select $V - K$ color we used the relationships between spectral type from Bessell & Brett (1988). We then converted from $V - K$ to 2MASS K_S using the color transformation from Carpenter (2001). The bolometric luminosity was then calculated using the observed K_S magnitude.

We also calculated the projected separation for our companions assuming the mean distance to Upper Sco, 145 ± 2 pc (de Zeeuw et al. 1999), and its depth on the sky, resulting in a final distance of 145 ± 15 pc. Furthermore, we ignored extinction in Upper Sco because the extinction is small for all of our objects ($A_V \lesssim 1$), and thus should not significantly affect the companion properties derived from the NIR spectra.

Finally, we searched for signatures of disks using *WISE* photometry (Wright et al. 2010) of the primary stars. Luhman & Mamajek (2012) suggests that 2MASS (K_S) and *WISE* ($W3$ and/or $W4$) photometry can differentiate stars with disks from those without disks. Stars of spectral type earlier than M4 with $K_S - W3 \gtrsim 1$ and $K_S - W4 \gtrsim 1$ should have a disk. They may also show a wider range of luminosities, due to thermal emission from the disk contaminating the K_S magnitudes used to compute M_{bol} . We found evidence for a debris/evolved transitional disk around the USco 1612–1800 system and marginal evidence for a debris/evolved transitional disk around USco 1610–1913. The other three systems showed no evidence for a disk.

Table 2 tabulates the photometry, the spectral type and the final derived physical properties for the five new companions and their primaries. Figure 8 shows the HR diagram for all previously known members of Upper Sco and our new companions. See Section 5 for discussion.

4.4. New Companions

Our spectroscopic observations of 13 candidates yielded five new companions. Four are new substellar companions with spectral types M9 (HIP 77900B), M9 (USco 1610–1913B), M8.5 (USco 1612–1800B), and M7.5 (USco 1602–2401B). One is a low-mass stellar companion with spectral type M5.5 (USco 1610–2502B). Figures 3, 4, 5, 6, and 7 show the UKIDSS K image and the reduced spectrum with the closest matching published spectrum for each of the companions. We describe them in more detail in the following sections.

4.4.1. HIP 77900B

HIP 77900 is a B6V star (Garrison 1967) with a model-dependent mass of $3.8^{+0.7}_{-0.5} M_\odot$ at 5 Myr ($3.8^{+0.8}_{-0.5} M_\odot$ at 10 Myr). Its membership in Upper Sco was first determined using both *Hipparcos* proper motions and parallax by de Zeeuw et al. (1999) and later by Rizzuto et al. (2011) with the addition of radial velocities.

Our new companion, HIP 77900B, has a projected separation of 3200 ± 300 AU and a spectral type of $M9 \pm 0.5$. The mass ratio between the primary for an age of 5 Myr, is $q = 0.005 \pm 0.002$ ($q = 0.005 \pm 0.003$ at 10 Myr). Mass ratios this small are rare but have been observed, such as for the HR 7329 system ($q \sim 0.01$; Lowrance et al. 2000) and HD 1160 ($q \sim 0.014$ for the B component; Nielsen et al. 2012). Although we have not determined if HIP 77900B is co-moving and bound to HIP 77900, its triangular H-band continuum confirms its youth and therefore membership in Upper Sco. Furthermore, Kraus & Hillenbrand (2008) found that binaries can be distinguished from chance alignments in Upper Sco at separations $\lesssim 75''$, down to primaries with $M \gtrsim 0.3 M_\odot$. The $22''$ separation of HIP 77900B suggests that it is truly associated with HIP 77900.

4.4.2. USco 1610–1913B

Preibisch et al. (2002) identified USco J161031.9–191305 (hereafter USco 1610–1913) as a member of Upper Sco based on lithium absorption ($EW[\text{Li}] = 0.55 \text{ \AA}$) and weak $H\alpha$ emission ($EW[H\alpha] = -2.3 \text{ \AA}$). Furthermore they determined a spectral type of K7 and $A_V = 1.1$ mag. At 5 Myr, USco J1610–1913 has a model-dependent mass of $0.88^{+0.14}_{-0.17} M_\odot$ ($0.87^{+0.11}_{-0.18} M_\odot$ at 10 Myr).

Kraus & Hillenbrand (2009b) determined that 2MASS 16103232-1913085 (hereafter USco 1610–1913B) and USco J1610–1913 are co-moving with a projected separation of 840 ± 90 AU. Using the flux ratio with the primary, Kraus & Hillenbrand (2009b) estimate a mass of $34 M_{Jup}$. The K magnitude ($K = 12.74 \pm 0.002$ mag) also suggests that the mass, assuming an age of 5 Myr, is $\approx 34 M_{Jup}$ and the spectral type is M7.8, using the methods described in Section 4.3. However we spectroscopically confirmed a later spectral type of $M9 \pm 0.5$. Assuming an age of 5 Myr, the model-dependent mass is $19^{+7}_{-4} M_{Jup}$ ($20^{+7}_{-3} M_{Jup}$ at 10 Myr), significantly lower than predicted from its absolute magnitude.

USco 1610–1913 has a small $K_s - W4$ excess (1.1 ± 0.2 mag), which is marginally consistent with the presence of a disk. However, there is no excess at $4.5 \mu\text{m}$, $8.0 \mu\text{m}$ or $24 \mu\text{m}$ (Luhman & Mamajek 2012), and thus there is likely no disk.

4.4.3. *USco 1612–1800B*

Preibisch et al. (2002) confirmed USco 161248.9–180052 (hereafter USco 1612–1800) as a member of Upper Sco based on lithium absorption ($EW[\text{Li}] = 0.52 \text{ \AA}$) and $H\alpha$ emission ($EW[H\alpha] = -3.8 \text{ \AA}$). They also determined the spectral type to be M3 with $A_V = 1.4 \text{ mag}$. Assuming an age of 5 Myr, the model-dependent mass is $0.36^{+0.14}_{-0.12} M_\odot$ ($0.36^{+0.14}_{-0.15} M_\odot$ at 10 Myr).

USco 1612–1800B has the smallest projected separation of our new companions ($430 \pm 40 \text{ AU}$). With a spectral type of M8.5, USco 1612–1800B has a mass of $23^{+12}_{-6} M_{Jup}$, assuming an age of 5 Myr ($26^{+16}_{-7} M_{Jup}$ at 10 Myr). Although it has not been confirmed as a comoving companion to USco 1612–1800, the spectrum shows signatures of youth consistent with its membership in Upper Sco and the small separation ($\sim 3''$) further implies that it is likely a bound system (Kraus & Hillenbrand 2008).

Although Luhman & Mamajek (2012) concluded that USco 1612–1800 has $W4$ excess and therefore hosts a debris/evolved transitional disk, USco 1612–1800 and USco 1612–1800B are separated by about $3''$, and thus unresolved by *WISE* (whose PSF FWHM range from $6\text{--}12''$). The 2MASS–*WISE* color is high, $K_s - W4 = 2.24 \pm 0.26 \text{ mag}$, but this represents the integrated light of the binary. We must deblend the $W4$ magnitude in order to conclude whether the primary or secondary has a disk. If we assume a typical $K_S - W4$ color for Upper Sco late-M stars with disks, ($K_S - W4 \approx 4\text{--}6 \text{ mag}$; Luhman & Mamajek 2012) we can estimate the $W4$ flux of the secondary to be $W4 = 7.2\text{--}9.2 \text{ mag}$. We also know that the secondary cannot be brighter than the integrated-light $W4$ magnitude of 8.1 mag . If there is a disk around the secondary, the resulting $K_S - W4$ for the primary is $K_S - W4 \lesssim 1.75 \text{ mag}$. This color still suggests that USco 1612–1800 may host a debris/evolved transitional disk but is also consistent with no disk. We conclude that there is likely a debris/evolved transitional disk in this system but cannot conclude if it resides around the primary or secondary.

4.4.4. *USco 1602–2401B*

2MASS J16025123–2401574 is a K4 member of Upper Sco (hereafter USco 1602–2401), identified as an X-ray source and spectroscopically confirmed by Kunkel (1999). At 5 Myr, the model-dependent mass is $1.34^{+0.12}_{-0.13} M_\odot$ ($1.18^{+0.06}_{-0.07} M_\odot$ at 10 Myr).

Kraus & Hillenbrand (2009b) confirmed that 2MASS J160251.16–240150.2 (hereafter USco 1602–2401B) is a co-moving companion to USco 1602–2401 with a projected separation of $1000 \pm 140 \text{ AU}$. USco 1602–2401B has a mass at 5 Myr is $41^{+20}_{-13} M_{Jup}$ ($47^{+20}_{-18} M_{Jup}$ at 10 Myr). This mass is significantly lower than the previous estimate, $\sim 0.11 M_\odot$, based on the flux ratio relative to the primary (Kraus & Hillenbrand 2009b).

The $K_S - W4$ color ($K_S - W4 \leq 0.98 \text{ mag}$) indicates that at most there is weak excess from any possible disk. However, Luhman & Mamajek (2012) find a $24 \mu\text{m}$ excess and conclude that USco 1602–2401 does have a debris/evolved transitional disk.

4.4.5. *USco 1610–2502B*

Preibisch et al. (1998) identified USco 161019.18–250230.1 (hereafter USco 1610–2502) as an X-ray source and determined its membership in Upper Sco based on lithium absorption ($EW[\text{Li}] = 0.52 \text{ \AA}$), $H\alpha$ emission ($EW[H\alpha] = -0.75 \text{ \AA}$). They also determined the spectral type to be M1. We find a model-dependent mass of $0.70^{+0.20}_{-0.20} M_\odot$ assuming an age of 5 Myr ($0.70^{+0.18}_{-0.17} M_\odot$ at 10 Myr).

Our new companion, USco 1610–2502B, is a confirmed proper motion companion to USco 1610–2502 (Kraus & Hillenbrand 2009b). It has a projected separation of $730 \pm 80 \text{ AU}$ and a model-dependent mass at 5 Myr of $0.10^{+0.08}_{-0.05} M_\odot$ ($0.09^{+0.07}_{-0.04} M_\odot$ at 10 Myr). Although its spectrum does not have the obvious triangular H-band continuum that distinguishes young ultracool dwarfs from older field objects, this feature is less pronounced for mid-M spectral types.

We find no evidence for a disk around USco 1610–2502 according to its 2MASS–*WISE* color, $K_s - W4 < 1.2 \text{ mag}$. Luhman & Mamajek (2012) also conclude that USco 1610–2502 has no disk because they detect no excesses at $4.5 \mu\text{m}$, $8.0 \mu\text{m}$, or $24 \mu\text{m}$. However, there is evidence for a disk around USco 1610–2502B according to its 2MASS–*WISE* colors, $K_s - W4 = 4.9 \pm 0.2 \text{ mag}$ and $K_s - W3 = 3.09 \pm 0.06 \text{ mag}$.

4.5. *Background Objects*

We identified a total of nine background objects (Table 1) and compared the NIR spectra with the IRTF/SpeX Prism Library to visually classify them. We also fit these objects with a reddened blackbody to determine if they were reddened early-type stars, i.e. background stars. Two of our background objects had flat spectra that could not be reproduced with a reddened blackbody and thus may be galaxies.

5. DISCUSSION

In Figure 8 we show an HR diagram with our newly identified companions, the free-floating Upper Sco members, and the Baraffe et al. (1998) and Chabrier et al. (2000) models. The Upper Sco free-floating members in this diagram are taken from Kraus & Hillenbrand (2007a), Slesnick et al. (2008), and Lodieu et al. (2008). Our substellar companions as a group have systematically higher bolometric magnitudes than the observed cluster sequence (Figure 1 and Figure 8). Within the uncertainties in effective temperature, USco 1610–1913 and USco 1602–2401B clearly have a higher bolometric luminosities than both the known members and the models. We note that there is one other previously known M8 member, 2MASS J162243.85–195105.7, that is also overluminous compared to the observed cluster sequence and the models though it may be a spectroscopic binary (Dahm et al. 2012).

Furthermore, the primaries of our substellar companions as a group are not overluminous compared to the models (Figure 8), suggesting that the primary and companion may not be coeval in all cases. Although higher mass ($\sim 0.1\text{--}1.5 M_\odot$) young binary systems appear coeval (Kraus & Hillenbrand 2009a), our results suggest that this may not be true for lower mass companions.

Finally, USco 1610–1913B is also more luminous

(~ 1.5 mag) than HIP 77900B despite having the same spectral type (M9). The primary, USco 1610–1913, is not overluminous compared to the models although it has marginal evidence for a disk (Section 4) which could contaminate the K -band magnitude, and hence the calculated bolometric luminosity.

One possible reason for the overluminosity of young companions compared to the models could be different accretion histories (Baraffe et al. 2012). Young stars may have strong episodic accretion which will increase the star’s radius and thus the luminosity. For example, Bowler et al. (2011) found that the planetary-mass companion GSC 06214-00210b in Upper Sco likely has strong accretion from a circumplanetary disk. Strong accretion could also explain the discrepancy of 1.5 mag between the luminosities of our two new M9 companions, HIP 77900B and USco 1610–1913B.

The wide projected separations of our new companions are difficult to explain as either the massive-end of gas-giant planet formation or the low-mass tail of binary-star formation. Binary star systems can have very wide separations up to several thousand AU (e.g. Duquennoy & Mayor 1991) but it is still unclear whether wide binaries can form with such an extreme separation (~ 3100 AU) and mass ratio (~ 0.005) as the HIP 77900AB system. However, even if they formed from a protoplanetary disk, planet formation has only been modeled to a few hundred AU (e.g. Kratter et al. 2010; Meru & Bate 2010). Thus, whether protoplanetary disks can also create such wide planetary-mass companions remains uncertain.

6. CONCLUSIONS

We have used PS1 and UKIDSS photometry to search for wide (≈ 400 – 4000 AU) planetary-mass companions in Upper Sco down to $\sim 5 M_{Jup}$. We use a selection method that combines traditional color-selection with SED fitting. Our method significantly decreases the number of reddened background stars that contaminate our sample compared with a solely color-selected sample.

We obtained followup low-resolution NIR spectroscopy of several candidates and discovered two new companions and confirmed three other companions. Four are very low mass substellar companions (spectral type M7.5–M9, mass ≈ 15 – $60 M_{Jup}$) and one is a low-mass star (spectral type M5, mass $\sim 0.1 M_{\odot}$). The most extreme object is HIP 77900B because of its very wide projected separation (3200 ± 300 AU) and very small mass ratio ($q \approx 0.005$).

Altogether, we have spectroscopically confirmed 4 wide substellar companions out of our search around 673 Upper Sco members. Our results indicate a frequency for wide (400–4000 AU) substellar companions down to $5 M_{Jup}$ of $\sim 0.6 \pm 0.3\%$. The wide projected separations for all of our companions are difficult to explain as either the massive-end of planetary formation or the low-mass tail of binary-star formation.

In addition, two of our companions (USco 1610–1913B and HIP 77900B) present another puzzle, because they have the same spectral type but luminosities that differ by 1.5 mag. Altogether, our companions suggest that young substellar companions, but not necessarily their respective primary stars, are overluminous compared to the models and the observed cluster sequence. As a result, our new companions do not all appear coeval with their primary stars on an HR diagram, in contrast to

results for young higher mass binary systems (Kraus & Hillenbrand 2009a).

Regardless of the formation scenario of these companions, we can use them as young spectral benchmarks to constrain evolutionary models. These new companions provide us with a unique glimpse into the early life of brown dwarfs. Further discoveries will improve our constraints on models and our understanding of planet/brown dwarf formation, the typical properties of these young systems, and their likely evolution.

KMA’s research was supported by the National Science Foundation under Grant No. 0822443. Any opinion, findings, and conclusions or recommendations expressed in this material are those of the authors’ and do not necessarily reflect the views of the National Science Foundation. ALK was supported by a Clay Fellowship and by NASA through Hubble Fellowship grant 51257.01, awarded by STScI. KMA and MCL were also supported by NSF Grant No. AST09-09222. We thank Brendan P. Bowler for obtaining some of the IRTF/SpeX data. We used data products from the UKIRT Infrared Deep Survey (UKIDSS). The Pan-STARRS 1 Surveys (PS1) have been made possible through contributions of the Institute for Astronomy, the University of Hawaii, the Pan-STARRS Project Office, the Max-Planck Society and its participating institutes, the Max Planck Institute for Astronomy, Heidelberg and the Max Planck Institute for Extraterrestrial Physics, Garching, The Johns Hopkins University, Durham University, the University of Edinburgh, Queen’s University Belfast, the Harvard-Smithsonian Center for Astrophysics, the Las Cumbres Observatory Global Telescope Network Incorporated, the National Central University of Taiwan, the Space Telescope Science Institute, and the National Aeronautics and Space Administration under Grant No. NNX08AR22G issued through the Planetary Science Division of the NASA Science Mission Directorate. We also use data products from the Two Micron All Sky Survey, which is a joint project of the University of Massachusetts and the Infrared Processing and Analysis Center/California Institute of Technology, funded by the National Aeronautics and Space Administration and the National Science Foundation. In addition, we use of data products from the *Wide-field Infrared Survey Explorer*, which is a joint project of the University of California, Los Angeles, and the Jet Propulsion Laboratory/California Institute of Technology, funded by the National Aeronautics and Space Administration. This research has also benefitted from the M, L, and T dwarf compendium housed at DwarfArchives.org and maintained by Chris Gelino, Davy Kirkpatrick, and Adam Burgasser. We also use the IRTF Prism Spectral Library housed at <http://pono.ucsd.edu/~adam/browndwarfs/spexprism> and maintained by Adam Burgasser. We have also made use of TOPCAT, an interactive tool for manipulating and merging tabular data. Finally, mahalo nui loa to the kama’āina of Hawaii’i for allowing us to operate telescopes on Mauna Kea. We wish to acknowledge the very significant cultural role Mauna Kea has within the indigenous Hawaiian community and that we are very fortunate to be able to conduct observations.

Facilities: IRTF (SpeX), UKIRT (UKIDSS), Pan-STARRS 1 (3π Survey).

APPENDIX

A. SED TEMPLATES

We characterized the PS1 and UKIDSS color-magnitude relations for cool and ultracool dwarf stars (spectral type M0–L0) using open cluster dwarfs from Praesepe and Coma Berenices, young open cluster dwarfs from Upper Sco, and field dwarfs with parallaxes. In order to increase the flexibility of our program to fit to a variety of spectral energy distributions (SEDs), we also use field dwarfs with optical+NIR SEDs but without parallaxes and separate our fitting procedure into two parts: spectral type and photometric distance. We then use the resulting templates to determine the spectral types and the photometric distances of our candidates.

A.1. Average Templates from Clusters

A.1.1. Open Cluster Dwarfs

Our template Praesepe and Coma Berenices members are selected from Kraus & Hillenbrand (2007b). Praesepe (~ 600 Myr) is located at a distance of 170 pc (Hambly et al. 1995) and Coma Berenices (~ 400 Myr) is at 90 pc (Casewell et al. 2006). We use the Praesepe and Coma Berenices members with $\geq 95\%$ membership probability, spectral type $\geq M0$, and good quality photometry (in i_{P1} , z_{P1} , or y_{P1}) in the PS1 3π survey DVO catalog. After applying our data quality cuts (see Section 2), in total we had 506 cluster dwarfs (spectral type M0–M5) with a mixture of PS1 magnitudes, i_{P1} , z_{P1} , or y_{P1} , and UKIDSS magnitudes, $ZYJHK$.

In order to create the SED templates for the Praesepe and Coma Berenices members as a function of spectral type, we computed the weighted average for the absolute magnitude for each half spectral subclass (i.e. M0, M0.5, etc). We remove the binary sequence by selecting the stars which are brighter than a simple quadratic line which runs above most of the data. After accounting for the binary sequence in this fashion, we compute a 0.48 mag scatter in the absolute magnitudes for a given spectral type. This dispersion is consistent with previous studies of the absolute magnitudes of M dwarfs (e.g. Bochanski et al. 2010; Dupuy & Liu 2012). The final SEDs are tabulated in Table 3.

A.1.2. Upper Sco Members

We also created SED templates from known Upper Sco members spanning spectral type M0 to L2. Earlier type objects were saturated in PS1 and/or UKIDSS. Just as for the open cluster dwarfs, we selected UKIDSS and PS1 photometry with our same data quality restrictions. The final SED templates are the weighted average of the absolute magnitudes for each half spectral subclass (i.e. M0, M0.5, etc). Note that the large errors reflect the known large spread in absolute magnitude seen in the known members of Upper Sco (e.g. Lodieu et al. 2008). In total, we used 404 Upper Sco members stars to create the final SEDs although a different numbers of primaries are used for each SED average magnitude because of the variable coverage by both UKIDSS and PS1. The final SEDs are tabulated in Table 4.

A.2. Templates of Individual Field M and L Dwarfs

The M, L & T dwarfs are from taken from the Faherty et al. (2009) and Leggett et al. (2010) ultracool dwarf catalogs and DwarfArchives.org. By separating our fitting routine into two parts (spectral typing and distance determination), we can use significantly more templates (a selection from ≈ 1000 known field dwarfs instead of from only about 100 that have parallaxes). This method also better encompasses the SED variation within a given spectral type. The average properties do not fully convey their diversity (e.g. Leggett et al. 2001). Furthermore, we use the SEDs of individual field dwarfs, rather than constructing average SEDs for each spectral type, as for cluster dwarfs, as the final SED templates. Thus, the uncertainty in the templates are just the actual measurement errors in the PS1 and UKIDSS magnitudes. In our analysis, we also exclude dwarfs which are known binaries or close binaries (81) and without at least 3 good quality measurements from UKIDSS or PS1 (see Section 2). Therefore, the final set of dwarfs used to determine the spectral type has 115 dwarfs. For this work, only objects with spectral type M9–L0 are tabulated in Table 5. Although our fit includes the entire library of field dwarfs we do not expect to find any late L or T dwarfs in this work. The colors and details of PS1 colors for L/T dwarfs is reserved for a later paper where those details will be discussed. L/T dwarf colors for UKIDSS are already reported in other papers (e.g. Leggett et al. 2001; Hewett et al. 2006).

Finally, in order to determine the absolute magnitude as a function of spectral type, we use the 30 ultracool dwarfs (spectral type M7 to L0) with parallaxes and good quality measurements (see Section 2) in PS1 and/or UKIDSS. Therefore, we only use these 30 dwarfs with parallaxes to determine absolute magnitude from spectral type but use the full library of field dwarfs (115) to determine the spectral type from the SED.

A.3. Final Library of SED Templates

The final SEDs used to perform the χ^2 fit for spectral type have at least three of the following: i_{P1} , z_{P1} , y_{P1} , Z , Y , J , H , or K . There are a total of 133 templates covering the spectral type range M0–L2, where 10 are averages from the cluster dwarfs (Table 3), 8 are from Upper Sco primary stars (Table 4) and 115 are field dwarfs (Table 5). Upper Sco free-floating cluster members fill the gap at M6–M8 (between the open cluster members in Praesepe and Coma

Berenices and field dwarfs) where the majority of our candidates may be; Brown dwarfs in Upper Sco are expected have spectral types greater than M7. We show the optical-NIR colors as a function of spectral type for final SED templates in Figure 9. The observed scatter in color as a function of spectral type highlights the importance of using several SED templates for each spectral type. Finally, we use the weighted average cluster dwarf SEDs and only 30 field dwarf SEDs (with parallaxes) for the absolute magnitude-spectral type relation which covers the spectral type range M0–L8 with a few gaps. In our analysis, this relationship is only used to convert from the fitted spectral type to absolute magnitude as a check on whether the photometric distance is consistent with Upper Sco membership. For example, objects which fit early-M dwarfs will generally be farther (taking into account the higher luminosities observed for young stars) than expected and, thus, can be flagged as background stars.

REFERENCES

- Allers, K. N., et al. 2007, *ApJ*, 657, 511
- Ardila, D., Martín, E., & Basri, G. 2000, *AJ*, 120, 479
- Baraffe, I., Chabrier, G., Allard, F., & Hauschildt, P. H. 1998, *A&A*, 337, 403
- Baraffe, I., Vorobyov, E., & Chabrier, G. 2012, *ApJ*, 756, 118
- Bessell, M. S., & Brett, J. M. 1988, *PASP*, 100, 1134
- Bochanski, J. J., Hawley, S. L., Covey, K. R., West, A. A., Reid, I. N., Golimowski, D. A., & Ivezić, Z. 2010, *AJ*, 139, 2679
- Boss, A. P. 2001, *ApJ*, 563, 367
- Bowler, B. P., Liu, M. C., Dupuy, T. J., & Cushing, M. C. 2010, *ApJ*, 723, 850
- Bowler, B. P., Liu, M. C., Kraus, A. L., Mann, A. W., & Ireland, M. J. 2011, *ApJ*, 743, 148
- Burgasser, A. J., Liu, M. C., Ireland, M. J., Cruz, K. L., & Dupuy, T. J. 2008, *ApJ*, 681, 579
- Burgasser, A. J., & McElwain, M. W. 2006, *AJ*, 131, 1007
- Burgasser, A. J., McElwain, M. W., Kirkpatrick, J. D., Cruz, K. L., Tinney, C. G., & Reid, I. N. 2004, *AJ*, 127, 2856
- Carpenter, J. M. 2001, *AJ*, 121, 2851
- Casali, M., et al. 2007, *A&A*, 467, 777
- Casewell, S. L., Jameson, R. F., & Dobbie, P. D. 2006, *MNRAS*, 365, 447
- Chabrier, G., Baraffe, I., Allard, F., & Hauschildt, P. 2000, *ApJ*, 542, 464
- Cushing, M. C., Vacca, W. D., & Rayner, J. T. 2004, *PASP*, 116, 362
- Dahm, S. E., Slesnick, C. L., & White, R. J. 2012, *ApJ*, 745, 56
- de Geus, E. J., de Zeeuw, P. T., & Lub, J. 1989, *A&A*, 216, 44
- de Zeeuw, P. T., Hoogerwerf, R., de Bruijne, J. H. J., Brown, A. G. A., & Blaauw, A. 1999, *AJ*, 117, 354
- Dodson-Robinson, S. E., Veras, D., Ford, E. B., & Beichman, C. A. 2009, *ApJ*, 707, 79
- Dupuy, T. J., & Liu, M. C. 2009, *ApJ*, 704, 1519
- . 2012, *ApJS*, 201, 19
- Duquenois, A., & Mayor, M. 1991, *A&A*, 248, 485
- Faherty, J. K., Burgasser, A. J., Cruz, K. L., Shara, M. M., Walter, F. M., & Gelino, C. R. 2009, *AJ*, 137, 1
- Garrison, R. F. 1967, *ApJ*, 147, 1003
- Golimowski, D. A., et al. 2004, *AJ*, 127, 3516
- Hambly, N. C., Steele, I. A., Hawkins, M. R. S., & Jameson, R. F. 1995, *A&AS*, 109, 29
- Hambly, N. C., et al. 2008, *MNRAS*, 384, 637
- Hewett, P. C., Warren, S. J., Leggett, S. K., & Hodgkin, S. T. 2006, *MNRAS*, 367, 454
- Ireland, M. J., Kraus, A., Martinache, F., Law, N., & Hillenbrand, L. A. 2011, *ApJ*, 726, 113
- Irwin, M. J., et al. 2004, in *Society of Photo-Optical Instrumentation Engineers (SPIE) Conference Series*, Vol. 5493, *Society of Photo-Optical Instrumentation Engineers (SPIE) Conference Series*, ed. P. J. Quinn & A. Bridger, 411–422
- Kaiser, N., et al. 2002, in *Society of Photo-Optical Instrumentation Engineers (SPIE) Conference Series*, Vol. 4836, *Society of Photo-Optical Instrumentation Engineers (SPIE) Conference Series*, ed. J. A. Tyson & S. Wolff, 154–164
- Kalas, P., et al. 2008, *Science*, 322, 1345
- Kenyon, S. J., & Hartmann, L. 1995, *ApJS*, 101, 117
- Kirkpatrick, J. D., Barman, T. S., Burgasser, A. J., McGovern, M. R., McLean, I. S., Tinney, C. G., & Lowrance, P. J. 2006, *ApJ*, 639, 1120
- Kirkpatrick, J. D., Henry, T. J., & McCarthy, Jr., D. W. 1991, *ApJS*, 77, 417
- Kirkpatrick, J. D., et al. 1999, *ApJ*, 519, 802
- . 2010, *ApJS*, 190, 100
- Kratter, K. M., Murray-Clay, R. A., & Youdin, A. N. 2010, *ApJ*, 710, 1375
- Kraus, A. L., & Hillenbrand, L. A. 2007a, *ApJ*, 662, 413
- . 2007b, *AJ*, 134, 2340
- . 2008, *ApJ*, 686, L111
- . 2009a, *ApJ*, 704, 531
- . 2009b, *ApJ*, 703, 1511
- Kraus, A. L., Ireland, M. J., Martinache, F., & Hillenbrand, L. A. 2011, *ApJ*, 731, 8
- Kunkel, M. 1999, PhD thesis, PhD Thesis Julius-Maximilians-Universität Würzburg (1999)
- Lafrenière, D., Jayawardhana, R., & van Kerkwijk, M. H. 2008, *ApJ*, 689, L153
- Lagrange, A.-M., et al. 2009, *A&A*, 493, L21
- Lawrence, A., et al. 2007, *MNRAS*, 379, 1599
- Leggett, S. K., Allard, F., Geballe, T. R., Hauschildt, P. H., & Schweitzer, A. 2001, *ApJ*, 548, 908
- Leggett, S. K., et al. 2010, *ApJ*, 710, 1627
- Lineweaver, C. H., & Grether, D. 2005, in *Protostars and Planets V*, 8252
- Lodieu, N., Hambly, N. C., & Jameson, R. F. 2006, *MNRAS*, 373, 95
- Lodieu, N., Hambly, N. C., Jameson, R. F., & Hodgkin, S. T. 2008, *MNRAS*, 383, 1385
- Looper, D. L., Burgasser, A. J., Kirkpatrick, J. D., & Swift, B. J. 2007, *ApJ*, 669, L97
- Lowrance, P. J., et al. 2000, *ApJ*, 541, 390
- Lucas, P. W., Roche, P. F., Allard, F., & Hauschildt, P. H. 2001, *MNRAS*, 326, 695
- Luhman, K. L., Burgasser, A. J., & Bochanski, J. J. 2011, *ApJ*, 730, L9
- Luhman, K. L., & Mamajek, E. E. 2012, *ApJ*, 758, 31
- Luhman, K. L., Stauffer, J. R., Muench, A. A., Rieke, G. H., Lada, E. A., Bouvier, J., & Lada, C. J. 2003, *ApJ*, 593, 1093
- Luhman, K. L., et al. 2006, *ApJ*, 649, 894
- Magnier, E. 2006, in *The Advanced Maui Optical and Space Surveillance Technologies Conference*
- Marois, C., Macintosh, B., Barman, T., Zuckerman, B., Song, I., Patience, J., Lafrenière, D., & Doyon, R. 2008, *Science*, 322, 1348
- Marois, C., Zuckerman, B., Konopacky, Q. M., Macintosh, B., & Barman, T. 2010, *Nature*, 468, 1080
- Martín, E. L., Delfosse, X., & Guieu, S. 2004, *AJ*, 127, 449
- Meru, F., & Bate, M. R. 2010, *MNRAS*, 406, 2279
- Muench, A. A., Lada, C. J., Luhman, K. L., Muzerolle, J., & Young, E. 2007, *AJ*, 134, 411
- Nielsen, E. L., et al. 2012, *ApJ*, 750, 53
- Preibisch, T., Brown, A. G. A., Bridges, T., Guenther, E., & Zinnecker, H. 2002, *AJ*, 124, 404
- Preibisch, T., Guenther, E., Zinnecker, H., Sterzik, M., Frink, S., & Roeser, S. 1998, *A&A*, 333, 619
- Rayner, J. T., Toomey, D. W., Onaka, P. M., Denault, A. J., Stahlberger, W. E., Vacca, W. D., Cushing, M. C., & Wang, S. 2003, *PASP*, 115, 362
- Rizzuto, A. C., Ireland, M. J., & Robertson, J. G. 2011, *MNRAS*, 416, 3108
- Schlafly, E. F., et al. 2012, *ApJ*, 756, 158
- Schmidt-Kaler, T. H. 1982, *Landolt-Bornstein Numerical Data and Functional Relationship in Science and Technology*, Vol. 2b, *Physical parameters of stars (Springer-Verlag)*, new Series, Group VI
- Siess, L., Dufour, E., & Forestini, M. 2000, *A&A*, 358, 593
- Skrutskie, M. F., et al. 2006, *AJ*, 131, 1163
- Slesnick, C. L., Hillenbrand, L. A., & Carpenter, J. M. 2008, *ApJ*, 688, 377
- Spiegel, D. S., Burrows, A., & Milsom, J. A. 2011, *ApJ*, 727, 57
- Taylor, M. B. 2005, in *Astronomical Society of the Pacific Conference Series*, Vol. 347, *Astronomical Data Analysis Software and Systems XIV*, ed. P. Shopbell, M. Britton, & R. Ebert, 29
- Tonry, J. L., et al. 2012, *ArXiv e-prints*
- Vacca, W. D., Cushing, M. C., & Rayner, J. T. 2003, *PASP*, 115, 389
- Vicente, S. M., & Alves, J. 2005, *A&A*, 441, 195
- Walter, F. M., Vrba, F. J., Mathieu, R. D., Brown, A., & Myers, P. C. 1994, *AJ*, 107, 692
- Wright, E. L., et al. 2010, *AJ*, 140, 1868

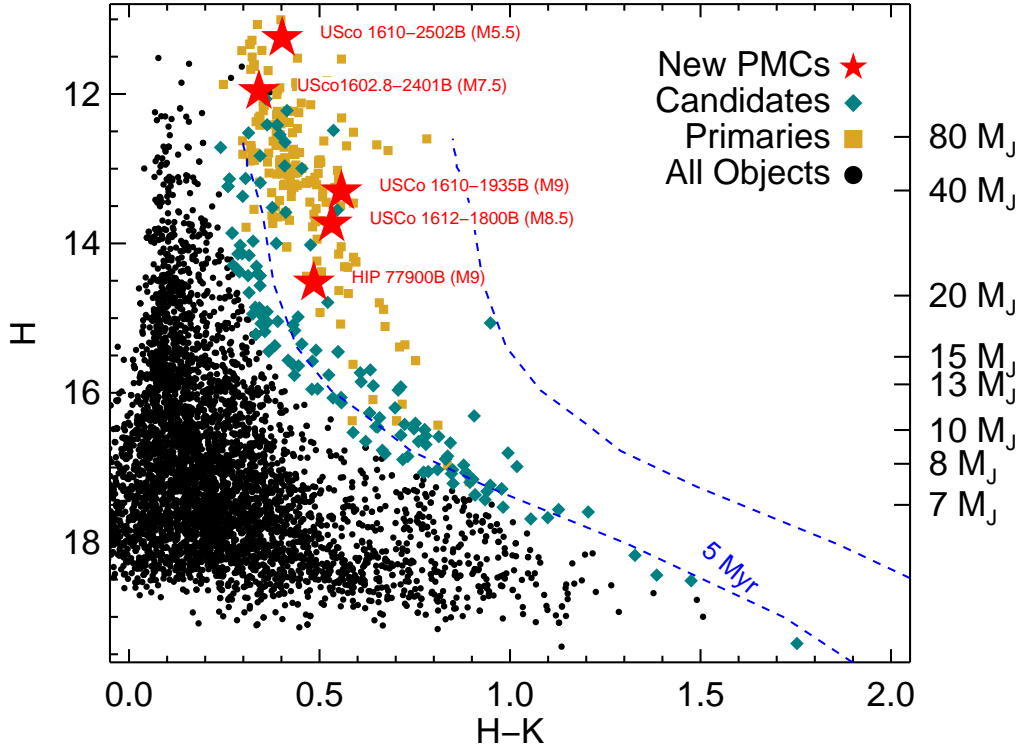


FIG. 1.— A color-magnitude diagram using the UKIDSS H and K magnitudes for all point sources within $\leq 30''$ of a known Upper Sco member. Known Upper Sco members are shown with orange squares and stand out from the background stars. The mass scale is shown using the Lyons/DUSTY evolutionary models (Chabrier et al. 2000) for a 5 Myr sequence (*right y-axis*) where the $H - K$ colors are given in the models. Our initial candidates (prior to the SED fit) are the teal diamonds which roughly follow the model sequence. The dashed *blue* lines outline the DUSTY 5 Myr sequence for Upper Sco where the two lines roughly encompass the observed spread in the sequence from the primary stars. The four new substellar companions (M7.5–M9, ~ 15 – $60 M_{Jup}$) and one new low-mass stellar companion (M5.5, $\sim 0.1 M_{\odot}$) are the *red stars*.

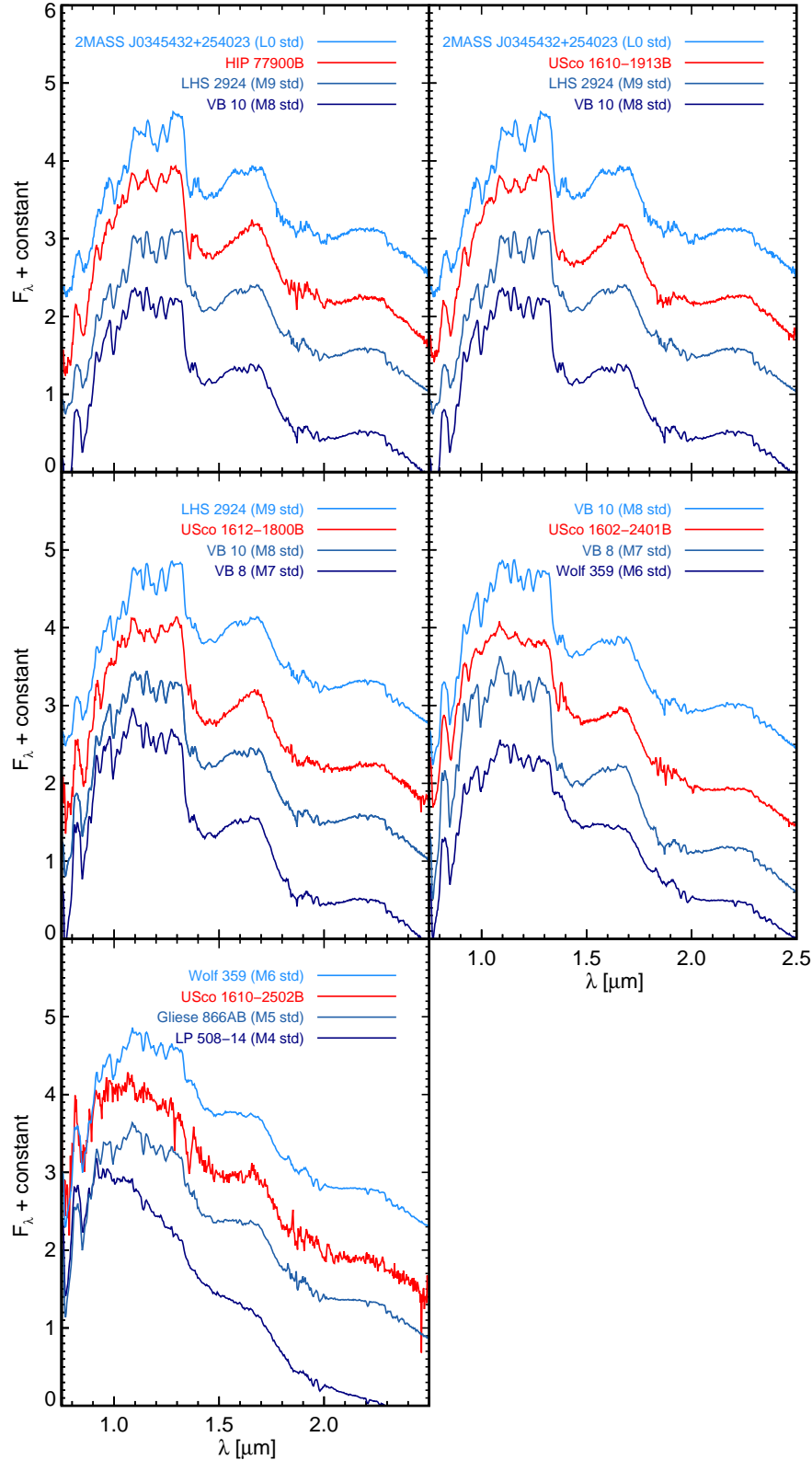


FIG. 2.— Comparison of our new companions to optical spectral standards for M dwarfs (Kirkpatrick et al. 1991) and L dwarfs (Kirkpatrick et al. 1999): LP 508-14 (M4, Burgasser et al. 2004), Gliese 866AB (M5, Burgasser et al. 2008), Wolf 359 (M6, Burgasser et al. 2008), VB 8 (M7, Burgasser et al. 2008), VB 10 (M8, Burgasser et al. 2004), LHS 2924 (M9, Burgasser & McElwain 2006), and 2MASS J0345432+254023 (L0, Burgasser & McElwain 2006). In the standards, the slope of both the H and K band continuum steadily changes from negative to positive with increasing spectral type. We determined the spectral type by visually comparing our companions with these standards according to the H and K continuum shape. We note that the spectra of the spectral standards and our young companions are not necessarily the same because of their age difference. The H -band continuum is notably triangular in young low-mass objects whose lower gravity leads to decreased H_2 collision induced absorption making the H_2O absorption more prominent (Lucas et al. 2001; Allers et al. 2007; Kirkpatrick et al. 2006). Our companions are plotted in the following order: HIP 77900B, USco 1610–1913B, USco 1612–1800B, USco 1602–2401B, USco 1610–2502B.

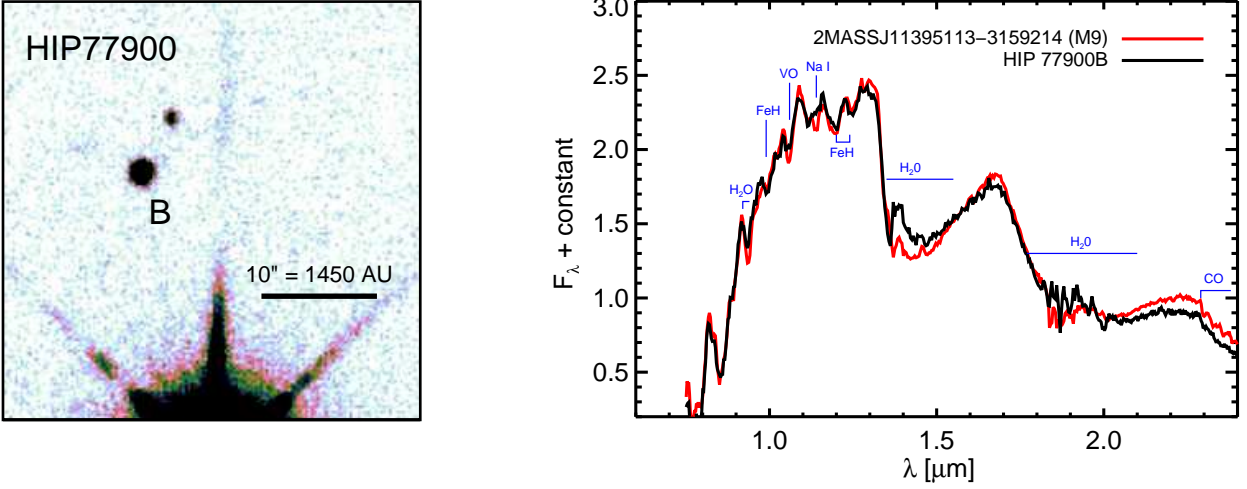


FIG. 3.— HIP 77900B has a projected separation of ≈ 3100 AU and a spectral type of M9 ($\approx 19 M_{Jup}$). *LEFT* – The finder chart (UKIDSS K and width of $30''$) with the letter B identifying the companion. North is *up* and East is *left*. *RIGHT* – IRTF SpeX spectrum of HIP 77900B compared to the young (8–12 Myr) M9 in TW Hyrae (Looper et al. 2007, 2MASS J11395113–3159214;).

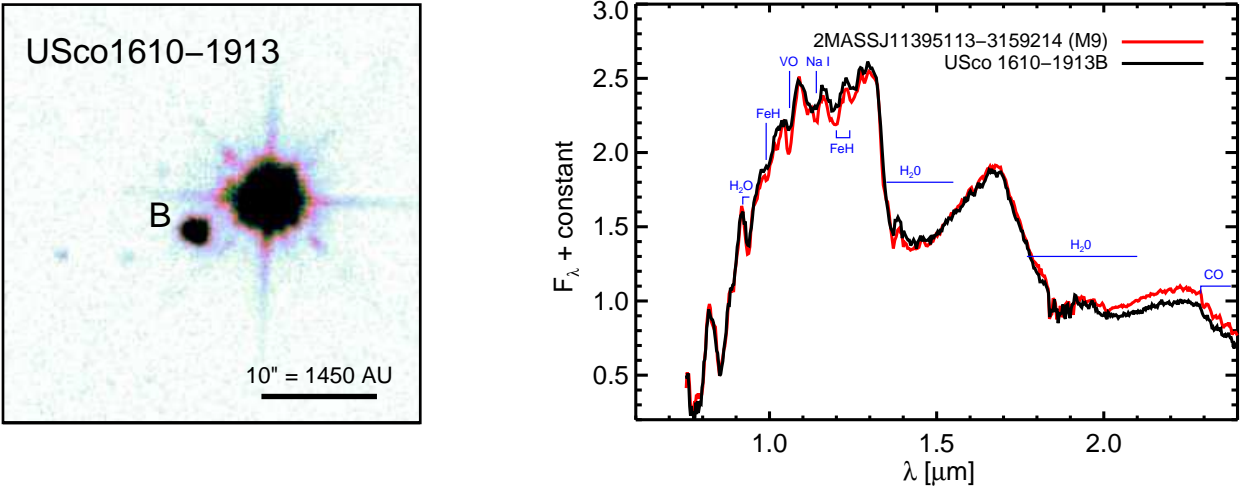


FIG. 4.— USco 1610–1913B has a projected separation of ≈ 800 AU and a spectral type of M9 ($\approx 19 M_{Jup}$). *LEFT* – The finder chart (UKIDSS K and width of $30''$) with the letter B identifying the companion. North is *up* and East is *left*. *RIGHT* – IRTF SpeX spectrum of USco 1610–1913B compared to the young (8–12 Myr) M9 in TW Hydrae (Looper et al. 2007, 2MASS J11395113–3159214;).

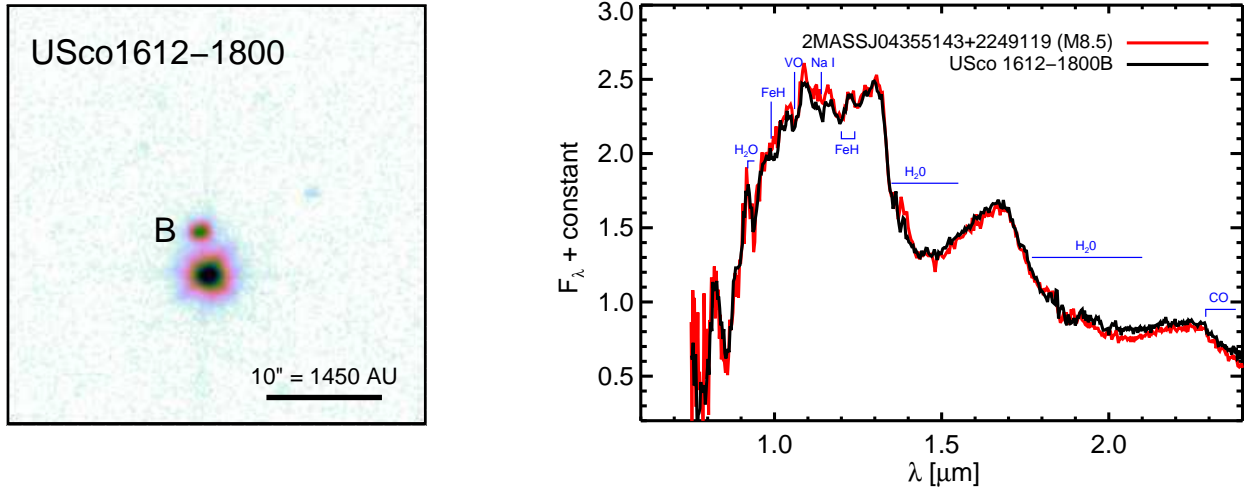


FIG. 5.— USco 1612–1800B has a projected separation of ≈ 400 AU and a spectral type of M8.5 ($\approx 23 M_{Jup}$). *LEFT* – The finder chart (UKIDSS K and width of $30''$) with the letter B identifying the companion. North is *up* and East is *left*. *RIGHT* – IRTF SpeX spectrum of USco 1612–1800B compared to the young (1–2 Myr) M8.5 in Taurus (2MASS J04355143+2249119; Muench et al. 2007).

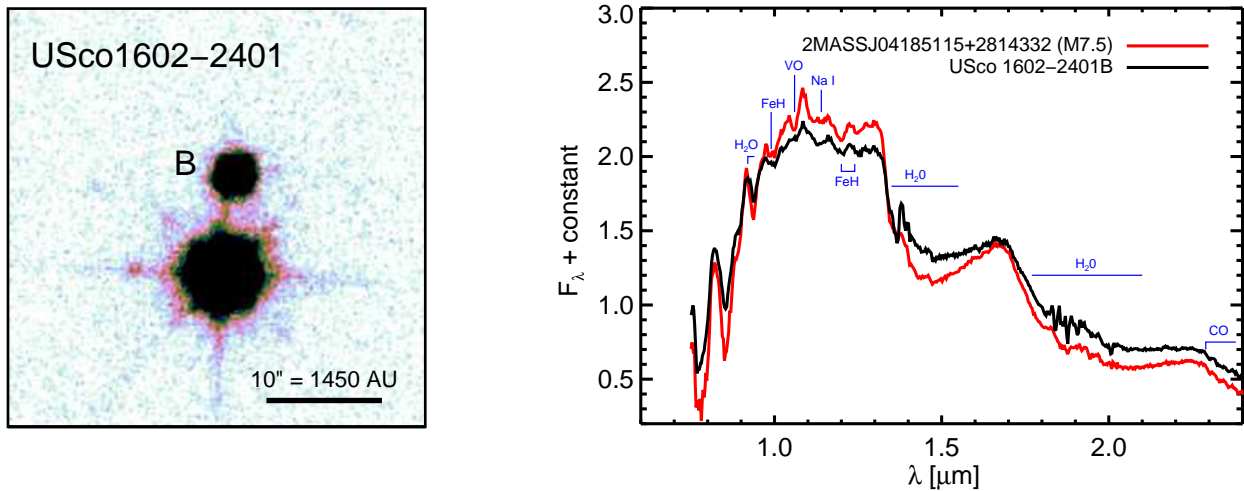


FIG. 6.— USco 1602–2401B has a projected separation of 1000 ± 14 AU and a spectral type of M7.5 ($\approx 41 M_{Jup}$). *LEFT* – The finder chart (UKIDSS K and width of $30''$) with the letter B identifying the companion. North is *up* and East is *left*. *RIGHT* – IRTF SpeX spectrum of USco 1602–2401B compared to the young (1–2 Myr) M7.5 in Taurus (2MASS J04185115+2814332; Muench et al. 2007).

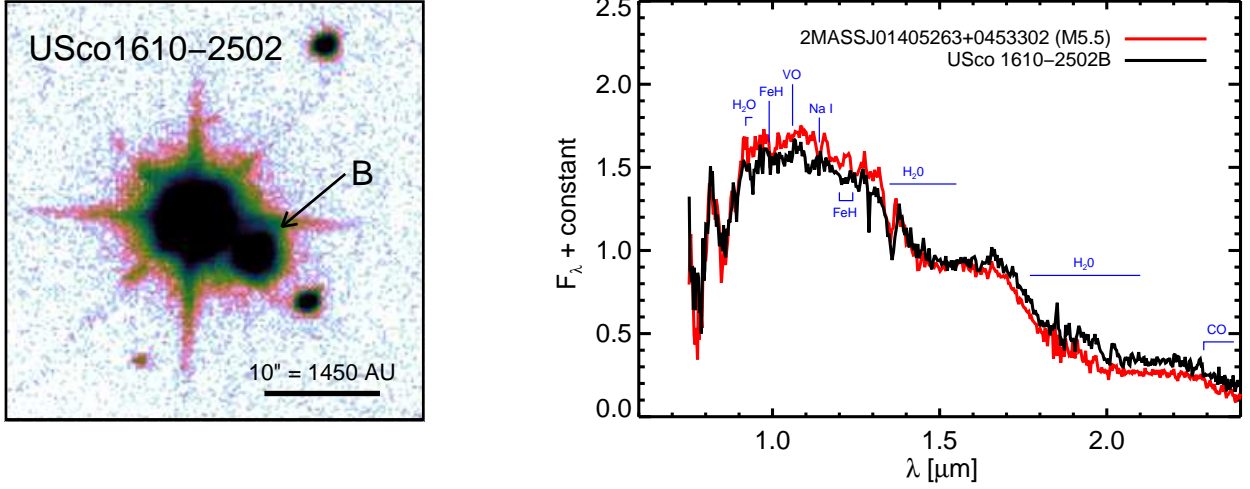


FIG. 7.— USco 1610–2502B has a projected separation of 732 ± 76 AU and a spectral type of M5.5 ($\approx 0.13 M_{\odot}$). *LEFT* – The finder chart (UKIDSS K and width of $30''$) with the letter B identifying the companion. North is *up* and East is *left*. *RIGHT* – IRTF SpeX spectrum of USco 1610–2502 compared to the field M5.5 (2MASS J04185115+0453302; Kirkpatrick et al. 2010).

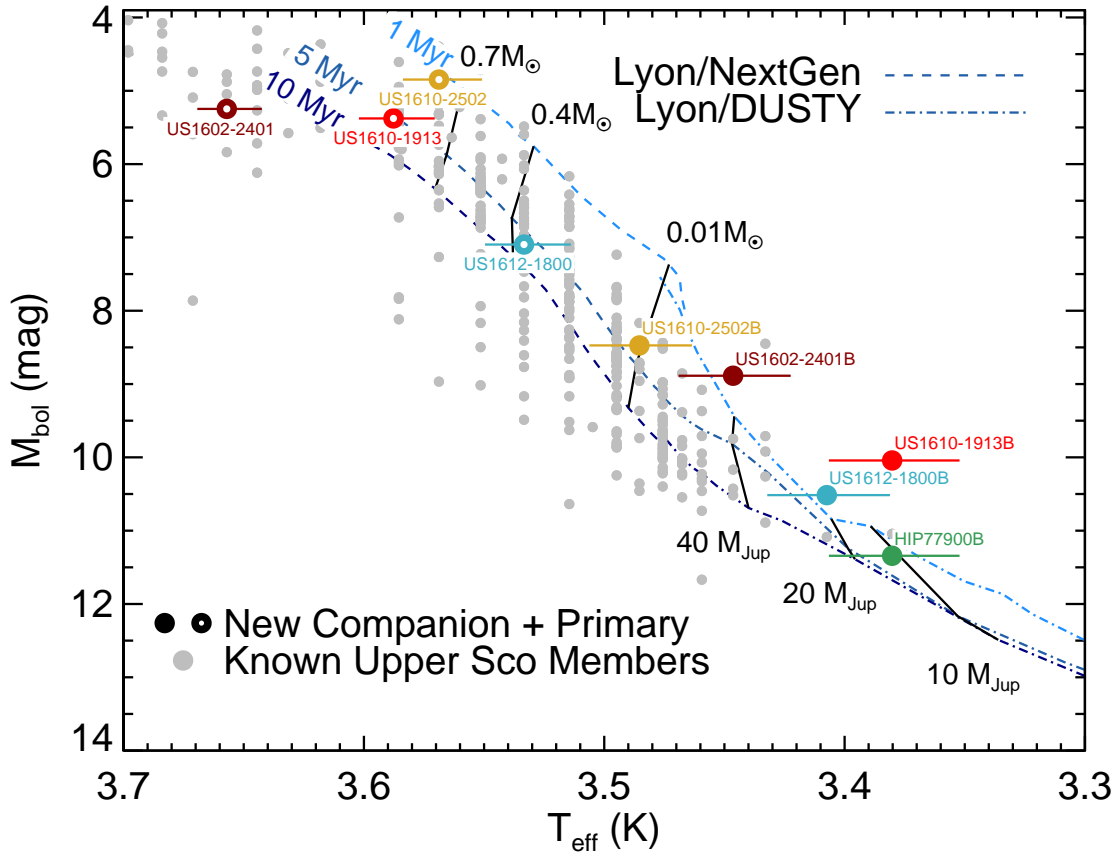


FIG. 8.— The bolometric luminosity and temperature of our new companions and their primaries compared to the model grids are the *solid* and *open circles* for the companions and the primaries, respectively (Chabrier et al. 2000; Baraffe et al. 1998). We omitted HIP 77900 because it has a very high mass and T_{eff} compared to the rest of the sample. Each system is represented by a different color. The *gray circles* are the Upper Sco free-floating members from Kraus & Hillenbrand (2007a). The three *dashed* colored lines are isochrones for 1 Myr (*light blue*), 5 Myr (*blue*), and 10 Myr (*dark blue*). The *solid black lines* trace out the evolution for an object with a given mass. The error bars for the uncertainty in bolometric magnitude, 0.13 mag, are smaller than the data points.

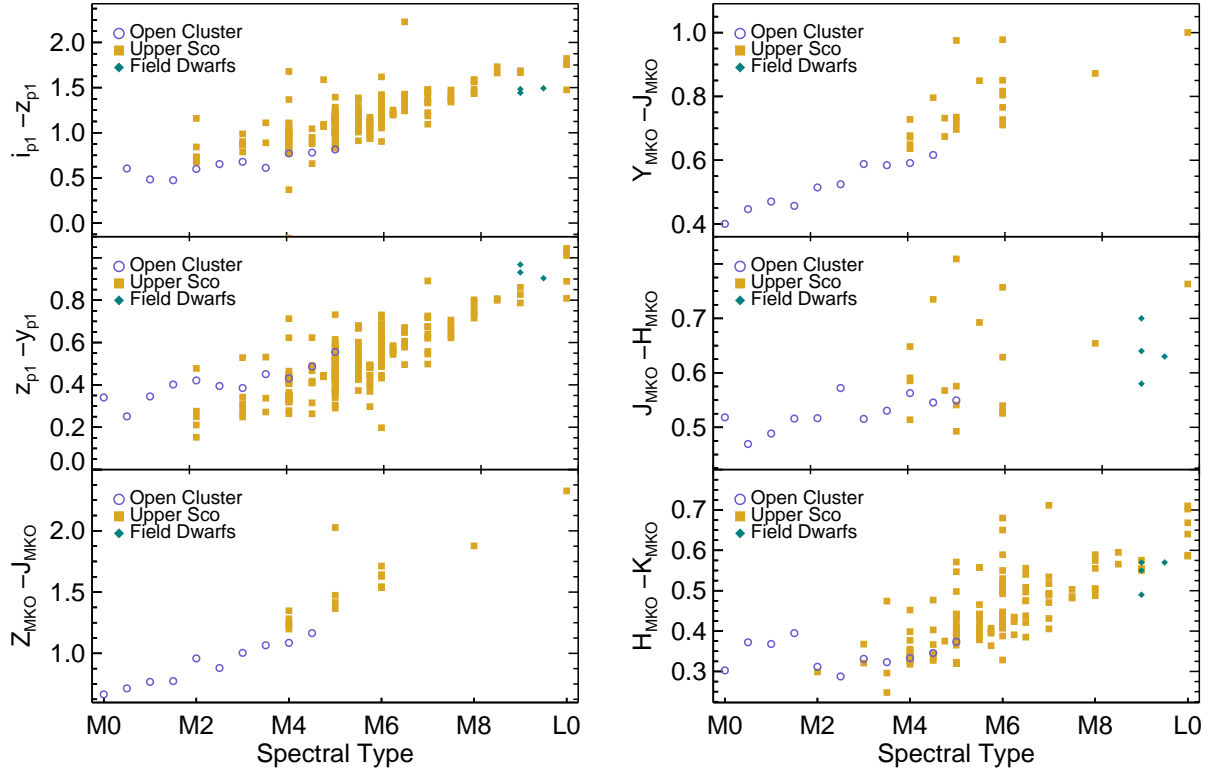


FIG. 9.— The optical and near-IR colors with i_{p1} , z_{p1} , y_{p1} , and the UKIRT $ZYJHK$ as a function of the spectral type for all the SED templates used in our spectral type routine. These templates all are constructed from individual objects with magnitude errors ≤ 0.2 mag and have detections in at least 3 filters (including one in the UKIDSS filters). The M dwarf templates constructed from averages from Praesepe and Coma Berenices members are the *purple open circles*. The individual SEDs from known Upper Sco M–L0 dwarf members are the *gold squares* and show the large spread in color in Upper Sco. The field dwarf SEDs are the *teal diamonds*.

TABLE 1
IRTF OBSERVATIONS

Name	RA (J2000)	Dec (J2000)	Date (UT)	T_{exp} (sec)	Spectral Type	Separation (arcsec)	PA (deg)	K (mag)	A0V Standard
New Candidates									
USco 1602–2401B	16:02:51.17	-24:01:50.45	2011 June 19	960	M7.5±0.5	7.0	352.1°	11.60±0.05 ^a	HD 145127
...	2013 April 16	360	HD 145127
USco 1610–1913B	16:10:32.33	-19:13:08.67	2011 June 19	720	M9.0±0.5	5.8	115.4°	12.74±0.01	HD 145127
...	2013 April 16	360	HD 144925
USco 1610–2502B	16:10:18.87	-25:02:32.78	2011 June 19	960	M5.5±0.5	5.1	239.3°	11.25±0.01	HD 145127
HIP 77900B	15:54:30.47	-27:19:57.51	2011 June 22	720	M9.0±0.5	21.8	12.7°	14.04±0.01	HD 146606
USco 1612–1800B	16:12:48.97	-18:00:49.56	2012 July 7	300	M8.5±0.5	3.0	11.0°	13.20±0.01	HD 144925
Background Objects									
HIP 78099-2B	15:56:48.53	-23:11:10.69	2011 June 20	960	reddened early-type star	12.4	132.0°	15.72±0.02	HD 145127
2MASS J16141484–24270844-6B	16:14:14.71	-24:27:06.23	2011 June 20	960	reddened M star	2.8	320.6°	15.24±0.02	HD 145127
USco 160936.5-184800-7B	16:09:36.51	-18:47:55.52	2011 June 21	600	reddened early-type star	5.5	356.7°	14.67±0.01	HD 138813
GSC06794-00537-18B	15:50:58.13	-25:45:28.05	2012 July 5	480	reddened early-type star	52.5	26.1°	17.95±0.19	HD 145188
USco 16213591–23550341-2B	16:21:35.37	-23:54:38.43	2012 July 5	480	reddened early-type star	26.3	343.5°	14.66±0.01	HD 144254
USco 161437.5–185824-0B	16:14:37.15	-18:58:43.13	2012 July 7	480	reddened early-type star	19.7	195.3°	16.14±0.03	HD 144925
USco 161437.5–185824-4B	16:14:35.87	-18:58:19.09	2012 July 7	480	reddened early-type star	24.0	282.1°	15.94±0.03	HD 144925
DENIS P J162041.5–242549-5B	16:20:42.34	-24:25:35.59	2012 July 8	480	reddened early-type star	18.3	41.9°	15.51±0.02	HD 142705
USco 160606.29–233513.3-1B	16:06:07.48	-23:34:57.16	2012 July 8	480	galaxy	22.9	45.3°	15.77±0.03	HD 142705

^a2MASS magnitudes used because UKIDSS photometry was unavailable.

^bThe ellipses (...) signify that the value is the same as in the row above.

TABLE 2
UPPER SCO NEW COMPANIONS

Property	HIP 77900B	USco 1610–1913B ^a	USco 1612–1800B	USco 1602–2401B ^a	USco 1610–2502B ^a
Directly Measured Properties					
RA (J2000)	15:54:30.47	16:10:32.33	16:12:48.97	16:02:51.17	16:10:18.87
Dec (J2000)	-27:19:57.51	-19:13:08.67	-18:00:49.56	-24:01:50.45	-25:02:32.78
Separation (AU)	3200 ± 300	840 ± 90	430 ± 40	1000 ± 140	730 ± 80
Primary Name	HIP 77900	USco 161031.9–191305	USco 161248.9–180052	USco 1602.8–2401	USco 161019.18–250230.1
Primary SpT ^b	B6±1	K7	M3	K4	M1
SpT	M9 ± 0.5	M9 ± 0.5	M8.5 ± 0.5	M7.5 ± 0.5	M5.5 ± 0.5
i_{P1} ^c	...	18.31±0.10	18.48±0.06	15.77±0.01	15.12±0.19
z_{P1} ^c	16.83±0.01	14.8±0.2	14.3±0.5
y_{P1} ^c	...	15.81±0.02	16.10±0.04	14.1±1.7	13.6±1.1
Z^c	16.86±0.01
Y^c	15.86±0.01
J^c	15.07±0.01	13.90±0.09 ^d	...	12.50±0.06 ^d	12.18± 0.06 ^d
H^c	14.52±0.01	13.30±0.01	13.73±0.01	11.97±0.01	11.65±0.01
K^c	14.04±0.01	12.74±0.01	13.20±0.01	11.60±0.05 ^d	11.25±0.01
$J - H$	0.54±0.02	0.53±0.06 ^d	0.60±0.01
$H - K$	0.49±0.02	0.56±0.02	0.53±0.04	0.37±0.05 ^d	0.40±0.01
$K_S - W4$	≤ 3.06 ^d	4.9±0.2
Primary $K_S - W4$	-0.26±0.09	1.1±0.2	2.2±0.3 ($\lesssim 1.8$) ^e	≤ 0.98 ^d	≤ 1.2
Derived Properties					
Primary M_{bol}	-0.72 ^{+0.20} _{-0.20} ^f	2.17 ^{+0.07} _{-0.07} ^f	2.40 ^{+0.13} _{-0.13} ^g	2.57 ^{+0.02} _{-0.02} ^f	0.93 ^{+0.12} _{-0.12} ^g
Primary T_{eff}	13700 ⁺¹⁵⁵⁰ ₋₁₂₀₀ ^f	4140 ⁺¹³⁰ ₋₁₆₀ ^f	3410 ⁺¹³⁰ ₋₁₅₀ ^g	4550 ⁺¹²⁰ ₋₁₄₀ ^f	3700 ⁺¹⁵⁰ ₋₁₄₀ ^g
Primary Mass (5Myr)	3.8 ^{+0.7} _{-0.5} ^f	0.88 ^{+0.14} _{-0.17} ^f	0.36 ^{+0.14} _{-0.12} ^g	1.34 ^{+0.12} _{-0.13} ^f	0.70 ^{+0.20} _{-0.20} ^g
Primary Mass (10Myr)	3.8 ^{+0.8} _{-0.5} ^f	0.87 ^{+0.11} _{-0.18} ^f	0.36 ^{+0.14} _{-0.15} ^g	1.18 ^{+0.06} _{-0.07} ^f	0.70 ^{+0.18} _{-0.17} ^g
M_{bol} ^h	11.38±0.13	10.09±0.13	10.52±0.13	8.87±0.13	8.47±0.13
T_{eff} ^h	2400 ⁺¹⁵⁰ ₋₁₅₀ (2390 ⁺¹³⁰ ₋₁₃₀)	2400 ⁺¹⁵⁰ ₋₁₅₀ (2400 ⁺¹⁴⁰ ₋₁₄₀)	2550 ⁺¹⁵⁰ ₋₁₅₀ (2450 ⁺¹⁴⁰ ₋₁₄₀)	2790 ⁺¹⁵⁰ ₋₁₅₀ (2550 ⁺¹⁵⁰ ₋₁₄₀)	3050 ⁺¹⁵⁰ ₋₁₄₀
Mass (5Myr) ⁱ	19 ⁺⁷ ₋₄ (18 ⁺³ ₋₃)	19 ⁺⁷ ₋₄ (19 ⁺⁴ ₋₃)	23 ⁺¹² ₋₆ (20 ⁺⁵ ₋₃)	41 ⁺²⁰ ₋₁₃ (24 ⁺⁸ ₋₄)	100 ⁺⁸⁰ ₋₅₀
Mass (10Myr) ⁱ	20 ⁺⁷ ₋₃ (20 ⁺⁴ ₋₂)	20 ⁺⁷ ₋₃ (20 ⁺⁴ ₋₂)	26 ⁺¹⁶ ₋₇ (20 ⁺⁶ ₋₂)	47 ⁺²⁰ ₋₁₈ (25 ⁺¹⁰ ₋₆)	100 ⁺⁷⁰ ₋₄₀

^aProper motion confirmed companion from Kraus & Hillenbrand (2009b).

^bSpectral type for HIP 77900 from Garrison (1967), for USco 1610–1913 and USco 1612–1800 from Preibisch et al. (2002), USco 1602.8–2401 from Kunkel (1999), and USco 1610–2502 from Preibisch et al. (1998).

^cFor all magnitudes we assume a minimum magnitude error of 0.01 mag (see Section 2). The ellipses (...) are used if no detection in that filter was available.

^d2MASS magnitudes used because UKIDSS photometry was unavailable.

^e K_S and *WISE* photometry is of the primary due to unresolved separation, $\sim 3''$. In this case, the K_S is likely accurate since it agrees well with the UKIDSS photometry (which resolves the primary and companion). In parenthesis is the lower limit to the $K_S - W4$ color assuming the typical $K_S - W4$ color range for an M7.5 (Luhman & Mamajek 2012) to extract its expected $W4$ magnitude.

^fThe uncertainties for HIP 77900 result from an assumed spectral type uncertainty of ± 1 subclass. Mass uncertainties in USco 161031.9–191305, USco 1602.8–2401, and USco 161248.9–180052 include 124 K temperature uncertainty from the spectral type conversion and an assumed spectral type uncertainty of half a subclass. We derive M_{bol} using bolometric corrections relationship to spectral type from Schmidt-Kaler (1982), T_{eff} , and mass derived using the Siess et al. (2000) evolutionary models. See Section 4 for details.

^gMass derived with the T_{eff} and the Baraffe et al. (1998) evolutionary models. The mass derived using the Luhman et al. (2003) temperature scale. The errors in the mass come from the uncertainty in temperature, which includes uncertainties due to spectral type and the conversion between spectral type and T_{eff} .

^h M_{bol} (uncertainty of 0.13 mag) is derived from empirical equations for the K bolometric correction from Golimowski et al. (2004). The T_{eff} is derived using the temperature scale for young stars (Luhman et al. 2003) where we assume an uncertainty of 124 K in this scale (same as in Golimowski et al. 2004). We also show T_{eff} from Golimowski et al. (2004), which was derived for older field ultracool dwarfs (uncertainty of 124 K), in parenthesis. The final uncertainty in T_{eff} includes uncertainties due to spectral type and the conversion between spectral type and T_{eff} .

ⁱMass derived with the T_{eff} and models from Chabrier et al. (2000). The mass derived using the Golimowski et al. (2004) temperature scale is in parenthesis. The errors in the mass come from the uncertainty in temperature and spectral type. For USco 1612–1800B and USco 1610–1913B the lower limit on the mass may be underestimated because it is extrapolated from the spectral type upper limit (M9.5) which is outside the Luhman et al. (2003) temperature scale (only M0–M9). Note for USco 1610–2502B we use the Baraffe et al. (1998) evolutionary models for the mass. See Section 4 for details.

TABLE 3
AVERAGE SEDS FOR CLUSTER DWARF STARS

Spectral Type	i_{P1} (AB)	z_{P1} (AB)	y_{P1} (AB)	Z (Vega)	Y (Vega)	J (Vega)	H (Vega)	K (Vega)
M0	...	7.70±0.16 (10)	7.4±0.3 (12)	6.8±0.3 (12)	6.5±0.3 (12)	6.12±0.19 (11)	5.60±0.08 (3)	5.30±0.19 (11)
M0.5	8.36±0.06 (3)	7.75±0.18 (13)	7.5±0.2 (16)	6.99±0.19 (15)	6.72±0.17 (13)	6.3±0.18 (15)	5.81±0.12 (3)	5.43±0.17 (17)
M1	8.58±0.15 (19)	8.1±0.2 (26)	7.8±0.3 (31)	7.2±0.3 (32)	7.0±0.3 (29)	6.5±0.2 (25)	5.99±0.11 (13)	5.6±0.3 (32)
M1.5	8.9±0.2 (27)	8.4±0.3 (36)	8.0±0.4 (36)	7.5±0.4 (38)	7.2±0.3 (32)	6.8±0.3 (33)	6.2±0.2 (23)	5.9±0.4 (39)
M2	9.2±0.4 (19)	8.6±0.3 (23)	8.2±0.5 (23)	7.9±0.5 (20)	7.5±0.4 (19)	6.9±0.4 (20)	6.4±0.3 (16)	6.1±0.4 (24)
M2.5	9.5±0.5 (34)	8.9±0.5 (40)	8.5±0.5 (36)	8.2±0.4 (34)	7.8±0.4 (30)	7.3±0.4 (29)	6.7±0.4 (31)	6.4±0.4 (40)
M3	9.9±0.4 (45)	9.3±0.4 (59)	8.9±0.4 (55)	8.5±0.4 (64)	8.0±0.4 (59)	7.5±0.3 (58)	6.9±0.4 (62)	6.6±0.4 (66)
M3.5	10.4±0.5 (64)	9.8±0.4 (76)	9.3±0.4 (75)	9.0±0.4 (81)	8.5±0.4 (76)	7.9±0.4 (70)	7.4±0.4 (81)	7.1±0.4 (87)
M4	11.1±0.6 (56)	10.4±0.5 (78)	9.9±0.5 (75)	9.6±0.4 (88)	9.2±0.3 (85)	8.6±0.3 (80)	8.0±0.3 (89)	7.7±0.4 (93)
M4.5	11.7±0.4 (45)	10.9±0.4 (57)	10.4±0.3 (57)	10.1±0.3 (62)	9.6±0.3 (60)	9.0±0.3 (58)	8.4±0.3 (60)	8.1±0.3 (63)
M5	12.26±0.01 (2)	11.45±0.07 (2)	10.89±0.01 (1)	8.90±0.01 (1)	8.53±0.01 (1)

NOTE. — The number of objects used to calculate the average magnitude in each filter given in parenthesis after the average magnitude. SEDs constructed from only one object often have very small photometric errors (we assume a minimum of 0.01 mag, see Section 2) whereas the other SEDs will have large photometric errors because of the observed large spread in absolute magnitude in young stars.

TABLE 4
AVERAGE SEDS FOR UPPER SCO PRIMARIES

Spectral Type	i_{P1} (AB)	z_{P1} (AB)	y_{P1} (AB)	Z (Vega)	Y (Vega)	J (Vega)	H (Vega)	K (Vega)
M0	8.8±0.2 (2)	7.88±0.04 (1)	8.00±0.3 (2)	5.81±0.01 (1)	...
M1	8.7±0.1 (1)	8.5±0.7 (2)	8.3±0.8 (2)
M2	9.6±0.5 (4)	8.98±0.19 (3)	7.7±0.8 (8)	6.5±0.4 (4)	6.70±0.01 (1)
M3	9.3±0.6 (11)	8.4±0.7 (7)	7.6±0.7 (19)	6.4±0.6 (5)	6.3±0.7 (3)
M3.5	9.7±0.7 (2)	8.7±0.6 (2)	7.8±0.6 (5)	7.33±0.01 (1)	6.57±0.01 (1)	5.98±0.01 (1)	6.06±0.01 (2)	5.6±0.2 (3)
M4	9.6±0.7 (32)	8.6±0.7 (32)	7.9±0.8 (48)	7.5±0.3 (6)	7.0±0.3 (5)	6.3±0.3 (5)	6.5±0.7 (21)	6.1±0.9 (17)
M4.5	9.7±0.8 (14)	8.7±0.8 (14)	8.0±0.8 (24)	...	7.9±1.0 (3)	7.2±0.9 (3)	6.7±0.6 (9)	6.2±0.7 (8)
M5	9.8±0.8 (66)	8.8±0.8 (67)	8.3±0.7 (71)	8.6±1.0 (4)	7.8±0.9 (4)	7.0±0.8 (4)	6.4±0.5 (53)	6.3±0.6 (26)
M5.5	10.3±0.7 (46)	9.2±0.7 (44)	8.7±0.6 (43)	...	7.26±0.01 (1)	6.41±0.01 (1)	6.6±0.5 (38)	6.4±0.5 (24)
M6	11.1±0.7 (43)	9.9±0.6 (42)	9.3±0.6 (43)	9.1±0.4 (5)	8.1±0.4 (9)	7.2±0.5 (7)	7.0±0.6 (41)	6.7±0.5 (34)
M6.5	11.7±0.6 (13)	10.2±0.6 (13)	9.7±0.6 (13)	7.4±0.6 (14)	7.1±0.5 (12)
M7	11.7±1.2 (16)	10.1±0.8 (14)	9.7±0.9 (16)	7.6±0.8 (13)	7.3±0.7 (11)
M7.5	12.1±0.7 (7)	10.6±0.6 (6)	10.0±0.6 (7)	7.8±0.4 (6)	7.1±0.3 (4)
M8	12.5±0.9 (7)	10.7±1.0 (8)	9.9±1.0 (8)	11.05±0.01 (1)	10.04±0.01 (1)	9.17±0.01 (1)	7.9±0.6 (6)	7.4±0.6 (6)
M8.5	13.7±0.3 (3)	11.80±0.01 (2)	11.2±0.2 (3)	8.6±0.2 (3)	8.02±0.18 (3)
M9	13.6±0.3 (2)	12.2±0.5 (3)	11.4±0.4 (3)	8.8±0.4 (3)	8.3±0.4 (3)
L0	15.3±0.6 (4)	13.9±0.7 (6)	13.0±0.6 (6)	12.17±0.01 (1)	10.84±0.01 (1)	9.84±0.01 (1)	10.0±0.6 (6)	9.3±0.6 (6)
L1	14.8±0.5 (2)	13.1±0.4 (2)	12.6±0.8 (3)	9.9±0.7 (4)	9.2±0.6 (4)
L2	...	13.2±0.11 (1)	12.21±0.01 (1)	9.31±0.01 (1)	8.63±0.01 (1)

NOTE. — The number of objects used to calculate the average magnitude in each filter given in parenthesis after the average magnitude. SEDs constructed from only one object often have very small photometric errors (we assume a minimum of 0.01 mag, see Section 2) whereas the other SEDs will have large photometric errors because of the observed large spread in absolute magnitude in young stars.

TABLE 5
SEDS FOR FIELD DWARF STARS

Name	Spectral Type	i_{P1} (AB)	z_{P1} (AB)	y_{P1} (AB)	Z (Vega)	Y (Vega)	J (Vega)	H (Vega)	K (Vega)
2MASS J08533619-0329321	M9	15.61 ± 0.01	14.13 ± 0.01		11.18 ± 0.05	10.48 ± 0.05	9.91 ± 0.05
2MASS J14284323+3310391	M9	...	14.89 ± 0.03	13.92 ± 0.01	...		11.91 ± 0.03	11.27 ± 0.03	10.72 ± 0.03
2MASS J15010818+2250020	M9	16.12 ± 0.01	14.67 ± 0.02	13.74 ± 0.01	...		11.76 ± 0.05	11.18 ± 0.05	10.69 ± 0.05
2MASS J00242463-0158201	M9.5	16.32 ± 0.01	14.83 ± 0.01	13.92 ± 0.03	...		11.73 ± 0.03	11.10 ± 0.03	10.53 ± 0.03
2MASP J0345432+254023	L0	18.50 ± 0.02	...	15.99 ± 0.01	...	15.32 ± 0.10	13.84 ± 0.05	13.20 ± 0.05	12.66 ± 0.05
SDSSp J225529.09-003433.4	L0	20.01 ± 0.07	17.00 ± 0.05		15.50 ± 0.05	14.80 ± 0.05	14.28 ± 0.05

NOTE. — We assume a minimum of $\sigma = 0.01$ mag for all photometry (see Section 2).